Accepted Manuscript

Design, Synthesis, and Biological Evaluation of Novel Thiazolidinediones as PPARγ/FFAR1 Dual Agonists

Khalid M. Darwish, Ismail Salama, Samia M. Mostafa, Mohamed S. Gomaa, Mohamed A. Helal

PII: S0223-5234(15)30435-9

DOI: 10.1016/j.ejmech.2015.12.049

Reference: EJMECH 8289

To appear in: *European Journal of Medicinal Chemistry*

Received Date: 19 August 2015

Revised Date: 27 December 2015

Accepted Date: 28 December 2015

Please cite this article as: K.M. Darwish, I. Salama, S.M. Mostafa, M.S. Gomaa, M.A. Helal, Design, Synthesis, and Biological Evaluation of Novel Thiazolidinediones as PPARγ/FFAR1 Dual Agonists, *European Journal of Medicinal Chemistry* (2016), doi: 10.1016/j.ejmech.2015.12.049.

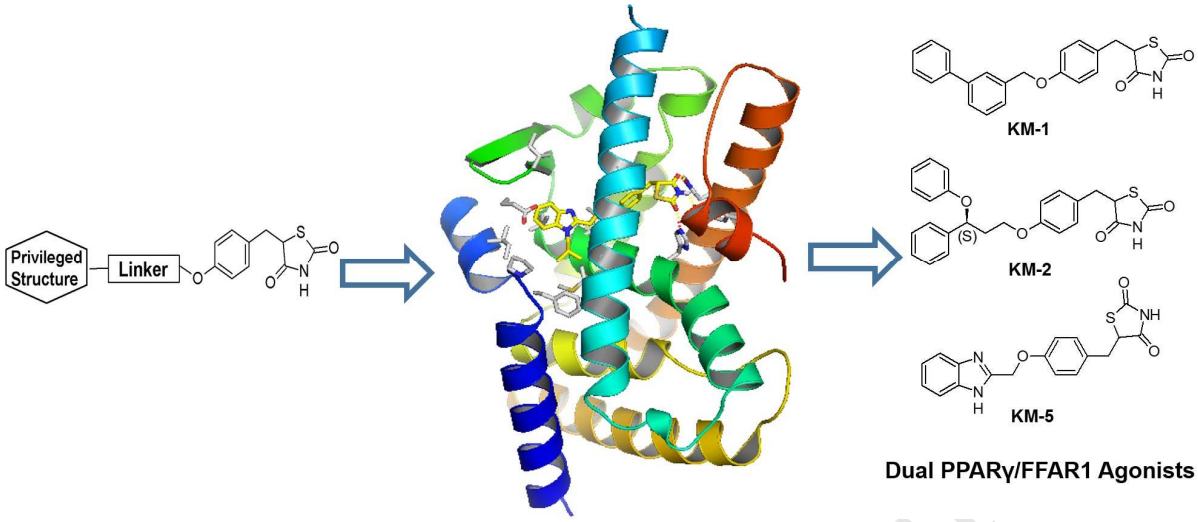

Design, Synthesis, and Biological Evaluation of Novel Thiazolidinediones as PPARγ/FFAR1 Dual Agonists

Khalid M. Darwish[a], Ismail Salama[a], Samia M. Mostafa[a], Mohamed S. Gomaa[a], and Mohamed A. Helal[a,*]

[a]Medicinal Chemistry Department, Faculty of Pharmacy, Suez Canal University, Ismailia 41522, Egypt.

Corresponding Author: Mohamed A. Helal
Tel: +201201122213
E-mail address: mohamed_hilal@pharm.suez.edu.eg

Abstract

Diabetes mellitus is a chronic metabolic disorder that affects more than 180 million people worldwide. Peroxisome proliferator activated receptors (PPARs) are a group of nuclear receptors that have been targeted by the thiazolidinedione (TZD) class of compounds for the management of type II diabetes. PPARγ is known to regulate adipogenesis and glucose metabolism. Another emerging target for the design of antidiabetic agents is the free fatty acid receptor 1 (FFAR1), previously known as GPR40. Agonists of this receptor were found to enhance insulin secretion in diabetic patients. It has been reported that some thiazolidinediones (TZDs) activate FFAR1 with micromolar potency. In this study, based on docking studies into the crystal structure of PPARγ and a homology model of FFAR1, nineteen compounds were designed, synthesized, and biologically tested for agonistic activity on both receptors. Nine compounds showed promising dual activity, with two compounds, **11a** and **5b**, having affinities in the low micromolar range on both targets. These molecules represent the first antidiabetic agents that could act as insulin sensitizers as well as insulin secretagogues.

Key words: Diabetes**,** PPARγ, FFAR1, Thiazolidinedione, Docking.

1. Introduction

Diabetes represents a major health concern, especially in developing countries. According to the World Health Organization (WHO), more than 180 million people worldwide have diabetes and this number is expected to reach 366 million in 2030. Half of diabetes-related death cases occur in people under the age of 70 and this number is expected to increase by more than 50% in the next 10 years.[1] Moreover, the number of diabetic patients is continuously increasing due to several factors including population growth, increased life expectancy, increased rates of obesity, and lack of physical activity.[2]

The most widely used antidiabetic medications are insulin secretagogues and insulin sensitizers. Examples of insulin secretagogues include sulfonylureas and meglitinides, while metformin and thiazolidinediones (TZDs) are insulin sensitizers. TZDs were introduced in the late 1990s as the first agents that control blood glucose level by acting on Peroxisome proliferator-activated receptors (PPARs).[3-5] These represent a group of nuclear receptors that control cellular metabolism through the modulation of gene expression.[6] There are three distinct subtypes of PPARs: PPARα, PPARδ, and PPARγ. Activation of PPARγ has been shown to regulate glucose homeostasis, cellular differentiation, apoptosis, and inflammatory responses.[7] Over the past few years, there has been an influx of new antidiabetic agents acting on a variety of cellular targets. Free fatty acid receptors (FFARs) are a family of G-protein coupled receptors (GPCRs) that act as fatty acid sensors and play a crucial role in glucose homeostasis. Recent studies have demonstrated that both dietary fatty acids and synthetic agonists can stimulate glucose-dependent insulin secretion by acting on FFAR1 highly expressed in pancreatic β-cells.[8, 9]

Several studies reported that modulation of PPARγ using TZDs was not efficient at controlling diabetes in some patients. This led to the use of combination therapies containing both insulin secreting and insulin sensitizing agents, such as Amaryl M® (glimepiride and

metformin) and glucovance® (glibenclamide and metformin).[10] These findings suggest the need for co-administration of insulin sensitizers and insulin secretagogues for the management of diabetes in some situations.

Interestingly, it has been reported that some TZDs activate FFAR1 expressed in human HeLa cells with micromolar potency.[11, 12] In 2007, Owman and co-workers exploited the TZD scaffold for the design of FFAR1 ligands by combining fatty acids substructures with TZD heads. Two of the synthesized compounds in this study showed activity in the micromolar range (compounds **A** and **B**, **Figure 1**).[13] In a recent study, 2,000 TZDs from the Merck compound collection were screened using the FLIPR assay in human GPR40-CHO cells. This led to the discovery of a partial agonist for GPR40 (compound **C**, **Figure 1**) possessing an EC_{50} of 0.5 μM. The initial GPR40 activity of this compound was improved after subsequent optimization. However, it was inactive in binding assays against all human PPARα, -δ, and -γ isoforms.[14]

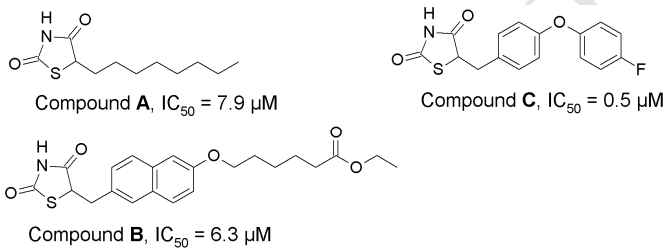

Figure 1: TZD-fatty acid hybrids

The objective of this study is to design and synthesize drug-like molecules with agonistic activity on both receptors; PPARγ and FFAR1. These agents would act as insulin sensitizers and insulin secretagogues through their action on PPARγ and FFAR1, respectively. The design of drugs with dual mode of action is a valid approach. Aleglitazar, a PPAR modulator with affinity for both PPARα and PPARγ, is currently in phase III clinical trials.[15] Similarly, Asenapine, a dual antagonist of dopamine D_2 and serotonin 5-HT_2 receptors, was launched in 2009 by Schering-Plough for the acute treatment of schizophrenia.[16] It is worth noting that

the endogenous ligands of both PPARγ and FFAR1 are fatty acids. Therefore, simultaneous activation of both PPARγ and FFAR1 should be well tolerated by the body, simulating the metabolic response after a fatty meal. Moreover, the concept of increasing insulin sensitivity and insulin secretion simultaneously has been successfully implemented using various marketed drug combinations as mentioned above.

2. Results and discussion

2.1. Compounds design

The basis for compound design was the similarity in structural requirements of the agonists of these two receptors. A careful literature survey revealed an evident similarity between the ligands reported for FFAR1 and those active on PPARγ.[17-19] A typical FFAR1 agonist consists of an acidic head attached to an aromatic scaffold, a heteroalkyl linker**,** and a hydrophobic tail. TZDs have very similar pharmacophoric features and are valid candidates for drug design because of their well-studied pharmacokinetics.[20-22] Representative examples of both FFAR1 agonists and PPARγ agonists are depicted in **Figure 2**. The design strategy was to combine the common 5-benzyl-thiazolidinedione head from TZDs with diverse hydrophobic fragments (tails). In a previous study, we illustrated through homology modeling and molecular dynamics simulations that the thiazolidinedione ring is capable of binding to the critical polar residues within both PPAR-γ and FFAR1 binding sites.[23]

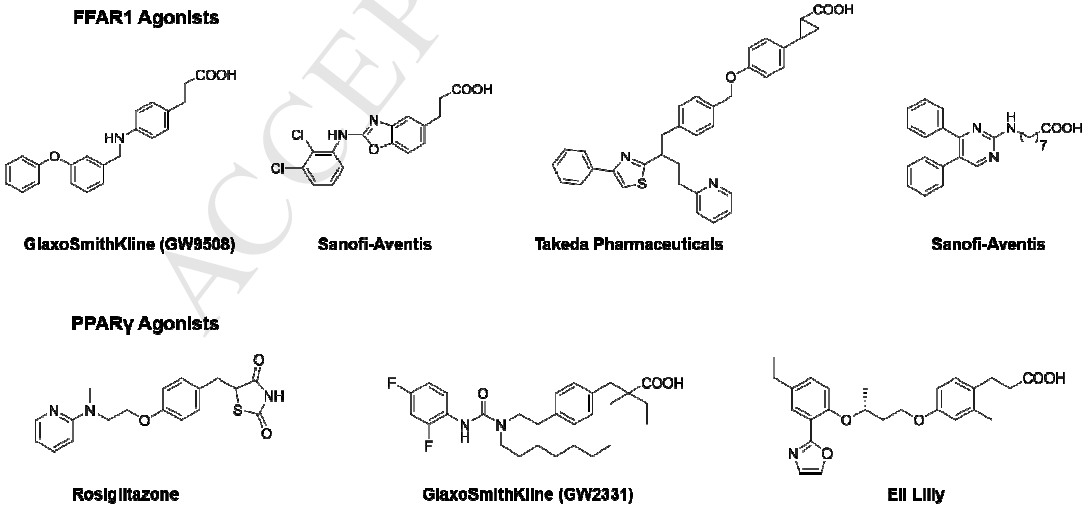

Figure 2: Representative examples of FFAR1 agonists and PPARγ agonists

Selection of the appropriate hydrophobic substructures was based on the "privileged structures" approach, which was introduced in the late 1980s by Evans and co-workers.[24] These structures can be defined as molecular scaffolds that bind with high affinity to multiple receptor families. To prove this concept, Bemis and Murcko performed an exhaustive analysis of all known drugs in the CMC database. This study revealed that the 5120 compounds in the CMC database contain 1179 different frameworks; however, only 32 (3%) of these frameworks account for 50% of all drugs.[25] An interesting example of the useful application of the privileged structures concept was reported in 1998. The 2-arylindole privileged molecular fragments were utilized as a starting point for the design of ligands for five different receptors; serotonin, melanocortin, chemokine, NPY, and neurokinin.[26] This phenomenon could be attributed to the presence of conserved regions deep in the binding site of most Class A GPCRs that are predominantly hydrophobic and recognized by the privileged structures. The previous findings suggest that empirically observed privileged structures are viable starting points for drug design, especially when targeting multiple receptors. Recently, there has been a large number of publications describing molecular frameworks considered as privileged structures for GPCRs.[27-32] In this study, the criteria for the selection of suitable privileged structures were; 1) similarity to previously reported FFAR1 and/or PPARγ agonists, 2) similarity to reported agonists for the purine receptor (which is the closest neighbor to FFAR1), 3) high frequency of occurrence among GPCR ligands.[33] Depending on these criteria, 17 fragments were selected (**Figure S1**, Supplementary Content) and utilized for the design of 17 initial scaffolds by combining these privileged structures with the 5-benzyl-thiazolidinedione head of TZDs through an ethoxy or methoxy linkers (**Figure 3**).

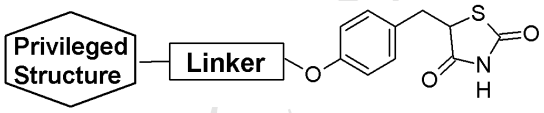

Figure 3: Design strategy of the dual PPARγ/FFAR1 agonists.

The 17 initial compounds were sketched, minimized, and docked into the ligand binding sites of FFAR1 and PPARγ. Docking studies were carried out using the co-crystal structure of PPARγ with rosiglitazone (PDB code: 3DZY) and the homology model of FFAR1 developed in our laboratory.[23] Careful examination of the binding sites of both receptors revealed an obvious similarity. Interestingly, both receptors had a hydrogen bonding triad at one end of the binding site and a Y-shaped hydrophobic pocket at the other end. This could explain, at least in part, the similarity between the agonists of FFAR1 and PPARγ. The

hydrogen bonding triad is formed by Arg183, Arg258, and Asn244 in FFAR1; and by His323, His449, and Tyr473 in PPARγ. Of the 17 docked compounds, 5 compounds showed satisfactory binding with both receptors (**Figure 4**). As expected, the thiazolidinedione ring formed hydrogen bonds with at least 2 of the 3 amino acid residues at the hydrogen bonding triad. In addition, the hydrophobic tail (privileged structure) showed favorable hydrophobic and π-π stacking interactions with the Y-shaped hydrophobic pocket of both FFAR1 and PPARγ (**Figure S2** and **S3**, Supplementary Content). It is worth noting that the biphenyl group in a meta arrangement (series **1**) made better hydrophobic contact with FFAR compared to its para counterpart. In addition, in terms of stereochemistry, our docking studies showed that the (S)-enantiomer of scaffold **2** ranked higher than its (R)-isomer. In this study, we decided to start a lead optimization campaign for three of these scaffolds; **1**, because of the reported importance of the biphenyl moiety for the FFAR binding; **2**, as a representative of the "branched biphenyl" chemotype; and **5**, as a representative for fused heterocycles.[34, 35] We selected **5** due to its similarity with rivoglitazone, a benzimidazole-based glitazone, which was reported in a recent study to be 3-times more active than rosiglitazone in a PPAR-γ transfection assay.[36]

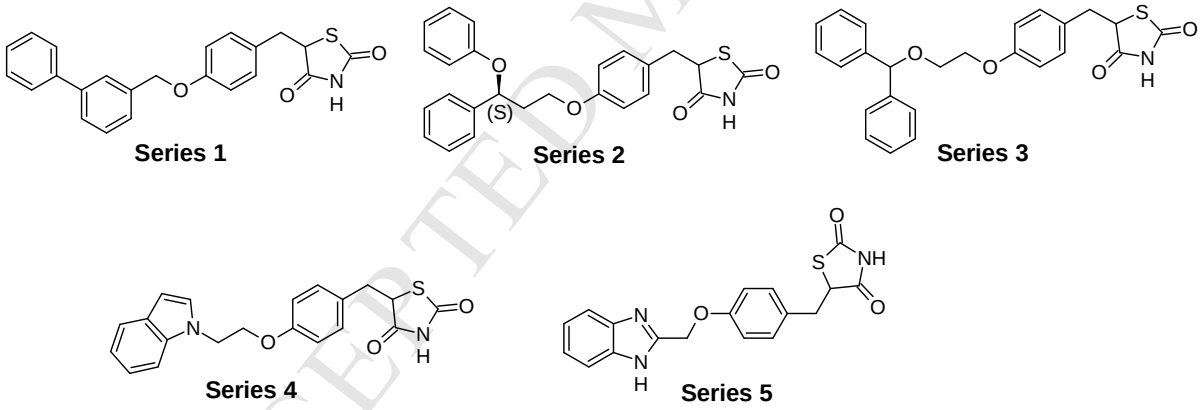

Figure 4: Scaffolds with the highest docking score in both FFAR1 and PPARγ.

2.2. Chemistry

The key thiazolidinedione head group was prepared by refluxing chloroacetic acid and thiourea in water for 12 h to yield pure white crystals of thiazolidine-2,4-dione after cooling (**Scheme 1**).[37] Subsequently, we attempted to synthesize the 5-(4-hydroxybenzylidene)-thiazolidinedione moiety first and attach the linker and the hydrophobic tail later on. This would allow us to introduce diversity at the last step of the synthesis. Unfortunately, the imide

group of the TZD head was found to interfere with the Mitsunobu coupling or nucleophilic substitution reactions required for installing the linker. In addition, the polarity of the 5-(4-hydroxybenzylidene)-thiazolidinedione moiety could complicate the purification step even if the problem of imide reactivity was tackled by protection/deprotection. Using this "forward" approach, only benzyl derivative **5** could be prepared in satisfactory yield (**Scheme 1**). Therefore, we decided to prepare all the designed compounds starting from the hydrophobic privileged structure, followed by the linker and 4-hydroxy benzaldehyde. Finally, Knoevenagel condensation with the TZD ring and reduction would furnish the target compounds (backward design).[38, 39]

Synthesis of the biphenyl-based series **1** was achieved using Suzuki-Miyaura cross-coupling (**Scheme 2**).[40] First, commercially available 3-bromobenzyl alcohol (**6a**) and 4-hydroxy benzaldehyde were coupled under Mitsunobu conditions to give the key benzyloxybenzaldehyde intermediate (**7a**). Second, Suzuki-coupling of this intermediate with the appropriate arylboronic acids provided the biaryl analogues (**8a-d**). Finally, Knoevenagel condensation with 2,4-thiazolidinedione followed by catalytic reduction using sodium borohydride/cobalt chloride-dimethylglyoxime (Co-DMG) complex provided the desired compounds in good yields.[41] In addition, we decided to exploit the size and lipophilicity of the bromine atom by synthesizing 3- and 4-bromophenyl derivatives instead of biphenyls. Compounds **11a** and **11b** were prepared using the appropriate bromobenzyl alcohols and the same procedure mentioned above but without the Suzuki coupling step (**Scheme 2**).

For the preparation of **2**, an asymmetric synthetic route was adopted by reducing the commercially available 3-chloropropiophenone **12** under Corey-Bakshi-Shibata (CBS) conditions using (S)-oxazaborolidine to furnish the enantiomerically pure alcohol (R)-(+)-3-chloro-1-phenyl-1-propanol.[42, 43] Then 4-hydroxybenzaldehyde was installed using Mitsunobu coupling to give the key intermediate alcohol **14**. This alcohol underwent

Mitsunobu coupling with the appropriate substituted phenols leading to compounds **15a-g** with inversion to the desired (S)-configuration.[44-46] These intermediates were condensed under Knoevenagel conditions with 2,4-thiazolidinedione to give benzylidenes **16a-g**. Reduction to the saturated 2,4-thiazolidinediones was accomplished using sodium borohydride and catalytic Co/DMG (**Scheme 3**). It is worth noting that the Y-shaped structures of these series could help the compounds to fit into the two hydrophobic arms of PPARγ and FFAR1, while maintaining a suitable size that is not too bulky.[9, 47, 48] Biological evaluation of series **1** and **2** enabled us to compare between straight and branched hydrophobic moieties and also gave insights into the binding preferences of FFAR1.

5 derivatives were prepared according to **scheme 4.** The benzimidazole ring was constructed using Phillips procedure by the condensation of phenylenediamine with glycolic acid in acidic medium to give compound **18**.[49] Alkylation of the NH of this intermediate with diverse alkyl halides was accomplished using sodium hydride in DMF. Then the resulting alcohol derivatives **19a-e** were coupled with 4-hydroxybenzaldehyde under Mitsunobu conditions to give aldehydes **20a-e**. Finally, condensation under Knoevenagel conditions with 2,4-thiazolidinedione followed by reduction using $NaHB_4$ and catalytic Co/DMG furnished the target compounds **5a-e**.

2.3. Biological evaluation

2.3.1. Human PPAR-γ Transactivation Assay

All the synthesized target compounds were tested for their ability to activate PPAR-γ using luciferase-based genetic reporter assay.[50] In this assay, mammalian cells were transfected with the ligand binding domain of PPAR-γ fused to a heterogonous DNA binding domain linked to the luciferase gene (**Figure S4,** Supplementary Content). The fold activation caused by test compounds was compared to a negative control sample of the vehicle DMSO. In addition, as a measure of intrinsic activity, the test compounds fold activation was also

calculated as a percentage of that of rosiglitazone (**Table 1**). Values ≥ 5-fold activation were considered statistically significant and may warrant further consideration.

As discussed above, this study focuses only on the modification of the lipophilic tail part because it is the moiety responsible for the unique pharmacodynamics of each glitazone. The bromophenyl and biphenyl derivatives caused moderate PPAR-γ transactivation activity with five compounds showing more than 5-fold activation. It was noticed that the biphenyl derivatives, **1a** and **1b**, were less active than the bromophenyl derivatives, **11a** and **11b**. This can be attributed to the rigidity of the biphenyl nucleus. Adding more bulk and rigidity using CF_3 group completely abolished the activity (**1d**). Unfortunately, series **MK-2** had modest activity with only compound **MK-2d** showing a 5-fold activation, perhaps due to the presence of the methoxy hydrogen bonding group which is able to make H bonding as well as hydrophobic contact with the binding pocket. In this series, 4 atoms separate the bulky biaryl tail from the core. This may push the terminal phenoxy group too far downwards into the receptor hydrophobic pocket. To our delight, four compounds of series **5** showed high PPAR-γ transactivation. The allyl derivative, **5c**, had higher intrinsic activity compared to rosiglitazone with 55-fold activation and an EC_{50} of 4.95 µM. Contrary to the **2** series, bulky substituents on the **5** scaffold, like the benzyl group in **5a**, were well tolerated by the receptor. It was reported that the presence of an H-bond acceptor in the hydrophobic tail may enhance the activity towards PPAR-γ.[51] This could be the reason for the improved activity of this series, together with the suitable size and shape of the benzimidazole privileged structure.

2.3.2. FFAR1 Calcium flux FLIPR Assay:

The target compounds were also tested for FFAR1 activation using calcium flux FLIPR assay (**Table 2**).[52] This study utilized a CHO-K1/FFA1/Gα15 stable cell line and a fluorometric imaging plate reader system (**Figure S5,** Supplementary Content). As expected, series **1** showed the highest activity towards FFAR1 in accordance with the reported biphenyl-

based FFAR1 agonists.[34, 35] Also, comparing *m*-Br and *p*-Br derivatives **11a** and **11b**, the meta arrangement was proved superior. **1c** is the most active compound in this series perhaps due to restricted rotation imparted by the two methyl groups in the ortho positions. Introduction of an H-bonding group, CF_3 in **1d**, did not significantly improve the activity. Series **MK-2**, the least active on PPAR-γ, showed moderate activity against FFAR1. The bulky α-phenoxy benzyl tail of this series seems to be more complementary to the FFAR1 hydrophobic pocket. Furthermore, increasing the steric bulk on ortho and/or para positions of the phenoxy group enhanced the activity as in compound **2g**. Again, the H-bonding group had little impact on the activity (compound **2e**). Fortunately, series **5**, the most active on PPAR-γ, showed acceptable activity on FFAR1 with the isobutyl derivative, **5b**, being the most active. Increasing the bulk of the substituent on the benzimidazole ring was well tolerated as the benzyl derivative, **5a**, showed good activity (4.11 μM). However, the cyclopentyl derivative was inactive perhaps due to its direct attachment to the benzimidazole scaffold that might hinder it from adapting the proper conformation.

2.4. Computational study

To examine the mode of binding and understand the structure-activity relationship of the synthesized ligands, all the compounds were docked into the crystal structures of PPARγ and FFAR1. To date, 138 crystal structures of human PPARγ have been reported and deposited into the Brookhaven protein data bank.[53] For the docking study, we used the crystal structure 3DZY because it is bound with rosiglitazone which possesses a similar pharmacophore to our compounds.[54] The Y-shaped cavity of PPARγ has two hydrophobic arms. The tighter and more hydrophobic arm I, which binds rosiglitazone, is formed by Met348, Ile281, Ile341, Leu228, Leu330, Leu353, and Val339. Arm II, lined with Ile326, Leu228, Leu330, Leu333 Phe226 and Glu295, is larger and relatively more hydrophilic. The TZD head of glitazones binds to the H bonding triad in the third arm which contains the important AF-2 helix. These

polar contacts stabilize the conformation of AF-2 that allows the binding of co-activator protein leading eventually to gene transcription.[55]

Our docking simulation study showed that series **1**, similar to rosiglitazone, binds to the more hydrophobic arm I. This might be due to the high lipophilicity of the biphenyl privileged structure which makes contacts with Ile281, Leu330, Val339, Ile341, Met348 and Leu353. **Figure 5a** shows the proposed binding mode of **1a** into the crystal structure of PPARγ. In addition to the lipophilic biphenyl moiety, central phenoxy group makes favourable contacts with Leu330 and Met364. However, the rigid nature of this series does not allow the TZD head, on the other end, to form the ideal H bonding network. Concerning series **2**, the docking poses of compound **2d** within PPARγ completely fills the lower arm II. Its terminal phenyl groups could efficiently make hydrophobic contacts with Phe226, Leu228, Ala292, and Met329. Its methoxy group is located close to both Glu295 and Glu343 with a good chance of forming water-mediated H bonds (**Figure 5b**). The overall orientation of this compound is similar to that of rosiglitazone but a bit lower to fill arm II. Unfortunately, the polar head of **2d** made H bond with His323 only and failed to interact with the other H bonding residues. In addition, the greatly reduced potency of **5e** and **5g** could be attributed to the bulky nature of the hydrophobic substituents that may cause steric clashes with the residues of the hydrophobic arm II. Finally, compound **5b**, which has balanced activity on both receptors, forms a near-perfect extensive network of H bonds with the key polar residues of the AF-2 helix of PPARγ, namely, His323, His449, and Tyr473. On the other end, its lipophilic part could make contacts with both hydrophobic arms. The benzimidazole moiety fits nicely in a tight pocket formed by Leu228, Leu330, and Leu333, while the isobutyl group extends downwards between Pro227 and Met329 without any steric clashes (**Figure 5c**). The previous observations emphasize the importance of H bonding interactions with the AF-2 helix for PPARγ activation. As a result, some of the prepared compounds showed obvious complementarity with the hydrophobic

cavity but failed to cause significant activation of the receptor due to the lack of H bonding with the critical polar residues.

As discussed before, a homology model of FFAR1, developed in our laboratory, was used for the design of our compounds library. However, during the course of our study, the crystal structure of FFAR1 in complex with the allosteric agonist TAK-875 was released.[56] Hence, we decided to use this crystal structure in the docking studies of the final compounds to question the possibility of binding of the prepared ligands to the observed allosteric site and compare the results to our previous docking and MD simulation study.[23] It is worth noting that the studied compounds were designed by docking them into the canonical orthosteric pocket among transmembrane helices (TM) 3, 5, and 7 as in other Class A GPCRs. In addition, prior to docking, this model had been subjected to MD simulation for 20 ns in an NPγT ensemble using Langevin dynamics with the agonist GW9508 in the orthosteric site. Compound GW9508 was selected because it is the most studied FFAR1 agonist and it lacks unnecessary functional groups. This previous simulation study helped to open up the putative binding site, break the ionic lock between Glu172 and Arg258, and transform the receptor into the active conformation.[23] However, the recently published crystal structure is bound to an allosteric ligand, TAK-875, binding in a pocket between TM3 and TM4 which is distinctive from the orthosteric site. In addition, contrary to our model, the whole receptor is in an "inactive-like" state with the ionic lock intact and TM7 close to the helical bundle core narrowing the putative binding site. Therefore, docking of our compounds into the FFAR1 crystal structure, with only one constrain to Arg258, led to the orientation of all ligands into the non-canonical site between transmembrane helices 3, 4, and 5 (**Figure 6**). Moreover, bulky compounds were found to protrude from the receptor between TM3 and TM4 in a similar fashion to the crystallized ligand TAK-875. On the other end, the TZD head of most of our

compounds were able to make H bonds with the critical polar residues of FFAR1; Arg183 and Arg258.

Series **1**, the most active against FFAR1, shows complete overlap with TAK-875 due to the similarity to the hydrophobic biphenyl tail of the crystallized ligand. We did not notice a significant effect of substitution on the terminal phenyl ring on activity. Similarly, it has been reported that the terminal phenyl ring of TAK-875 could accommodate variable substituents with negligible effect on the potency. These observations suggest an allosteric binding mode of series **1**, similar to the crystal structure, where the terminal substituents do not make contacts with the protein (**Figure 6a**). Likewise, series **2** adapts a binding mode in which the two phenyl rings protruding between TM3 and TM4. Within this series, we noticed that para-substitution is preferred to meta. Also, the ortho substitution in case of compound **2g** could rationalize its highest activity due to its ability to make hydrophobic interaction with Val84 (**Figure 6b**). However, the relatively weak activity of this series could be attributed to the sub-optimal H bonding network imparted by its bulky nature (weak interactions with Tyr91 and Arg258). Contrary to the other series, **5** shows a notable differential effect of substituents on the FFAR1 agonistic activity. This could be explained by the proximity of these substituents to the protein (**Figure 6c**). It is expected that the butyl and benzyl groups could make stronger hydrophobic interactions with Pro80, Val84, and Phe142 than the allyl and isopropyl groups. However, in case of **5e**, the combination of size, rigidity, and direct attachment of the cyclopentyl ring to the benzimidazole scaffold leads to loss of activity.

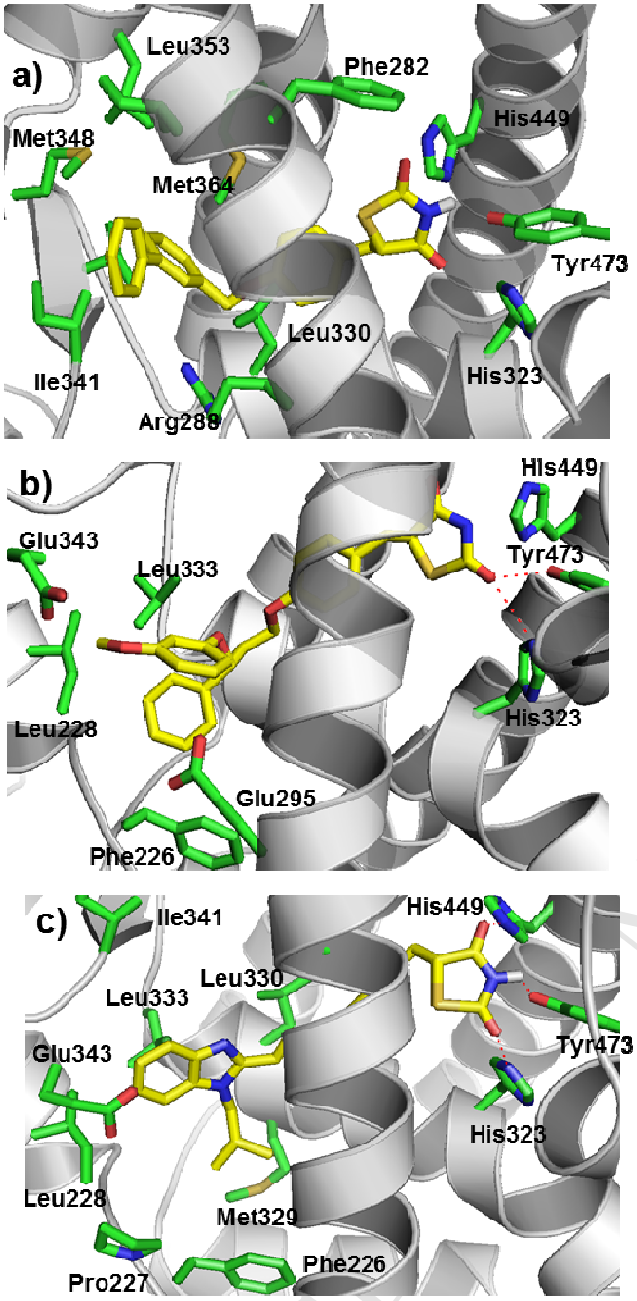

Figure 5: Proposed binding mode of **1a (a), 2d (b),** and **5b** in the crystal structure of PPARγ. Protein is represented as grey cartoon with amino acid residue colored green. Compounds are displayed as yellow sticks. Only residues having significant interaction with the ligand are shown.

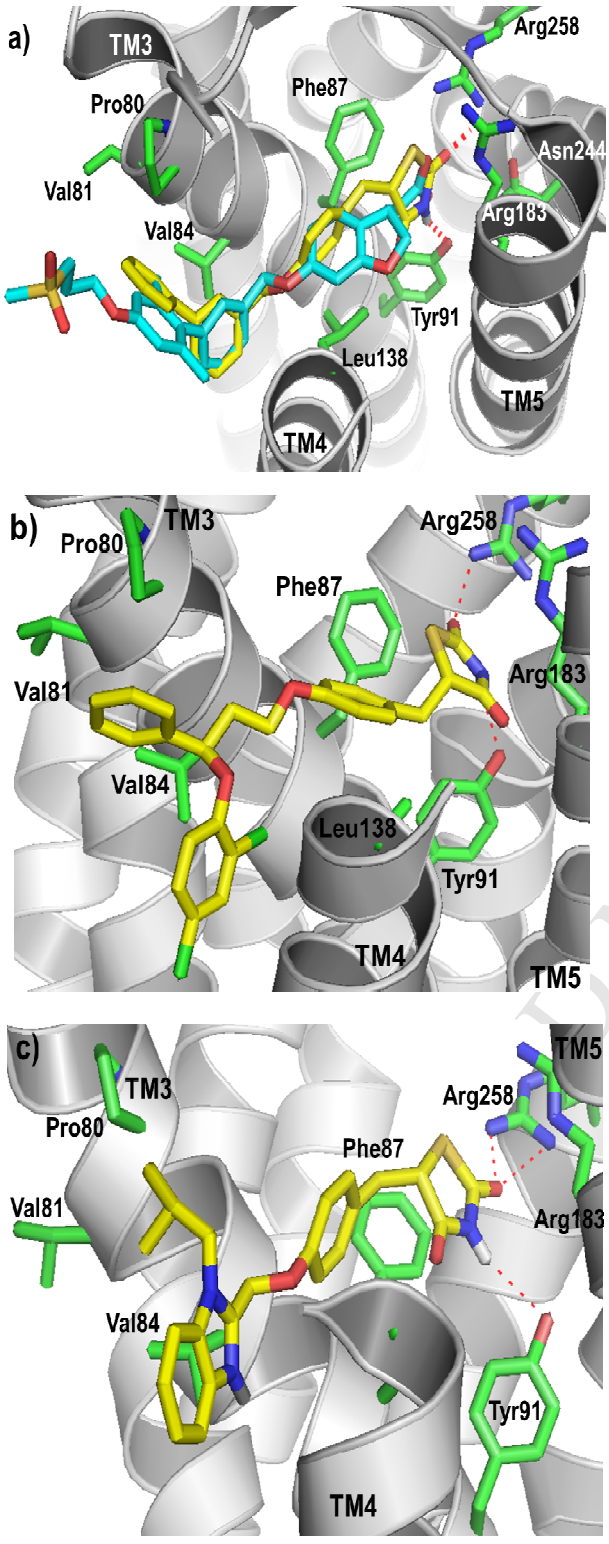

Figure 6: Proposed binding mode of **1a (a), 2g (b),** and **5b** in the crystal structure of FFAR1. Protein is represented as grey cartoon with amino acid residue colored green. The crystallized ligand TAK-875 (cyan) and the prepared compound (yellow) are displayed as sticks. A part of TM4 was removed for clarity.

3. Conclusions

TZDs represent a well-studied group of antidiabetic agents. Based on previous observations of the ability of some TZDs to activate FFAR1, we designed five scaffolds consisting of the TZD head, a linker, and a carefully selected privileged structure. For the present study, we decided to explore three of these scaffolds and nineteen compounds were synthesized. Nine of the prepared compounds showed acceptable activity on both receptors with series **5**, the benzimidazole-based series, being the most promising. Our docking study indicated that polar interactions with the H bonding triad of PPARγ or FFAR1 is more important for receptor activation than hydrophobic interactions. It should be emphasized that the main objective of this work was not to obtain a highly potent agonist on PPARγ or FFAR1, but to design a lead compound with a balanced activity on both targets. The benzimidazole series **5**, followed by the biphenyl series **1**, were proved to be the most suitable scaffolds for this purpose. They provide a privileged structure with suitable shape and size for further fine-tuning of the activity on both receptors. Future studies in our laboratory will aim to optimize these lead compounds as well as to explore the remaining scaffolds, **3** and **4**. We hope that these efforts could lead to the discovery of a dual acting antidiabetic agent to replace some of the currently used drug combinations.

4. Experimental

4.1. Chemistry

Reaction progress was monitored by thin layer chromatography (TLC) analysis on Merck silica gel 60 F254 plates. Visualization was performed with UV light (254 nm) or iodine. Yields are of purified compounds and were not optimized. Reagents and solvents were obtained from commercial sources and used without any further purification. Flash column chromatography was performed on Loba Chemie silica gel (200–400 mesh) as a stationary phase. Melting points (mp) were determined in open capillaries on an Electrothermal IA9100

melting point apparatus and were uncorrected. Optical rotations were measured with a JASCO, DIP-370 Digital polarimeter at 29 °C. Concentrations are expressed as g/100 ml. Low-resolution mass spectra (MS) were recorded with a Shimadzu QP2010-Plus gas chromatograph/mass spectrometer (GC/MS), electron impact (EI^+) 70 eV maintained at 250 °C. Infrared (IR) spectra were recorded on a Bruker Tensor 27 FT-IR spectrophotometer, driven by OPUSTM version 1.1 managing software (Vmax in cm^{-1}, using KBr pellets).

The proton and carbon nuclear magnetic resonance (^{1}H- and ^{13}C-NMR) spectra were recorded in $CDCl_3$ or DMSO-d_6 as a solvent on a Varian-MERCURY 300 (300 MHz) spectrometer or a Bruker Ascend Aeon 400 (400 MHz) spectrometer at room temperature within the range (20-25 °C). Chemical shifts (δ) are expressed as parts per million (ppm), using tetramethylsilane (TMS) as the internal standard. For Signal multiplicities, the following abbreviations are used as follows; s (singlet), d (doublet), dd (doublets of doublet), t (triplet), q (quartet), br s (broad singlet) and m (multiplet). Coupling constants (*J* values) are given in hertz (Hz). The acidic protons of the amidic –NH in the thiazolidindione ring, alcohols or aromatic amines were not frequently observed in ^{1}H-NMR spectra.

4.1.1. General Procedure A (Mitsunobu reaction).

To a stirred and ice-bath cooled mixture of the phenol (1 equiv) in anhydrous THF (9 ml), was added the alcohol (1 equiv). Triphenylphosphine (PPh3) (1.1 equiv) was added portionwise to this mixture and the system was kept under nitrogen by evacuation and filling with nitrogen three times. Subsequently, diisopropyl azodicarboxylate (DIAD) (94 wt % solution in toluene, 1.1 equiv) was added in a strictly dropwise fashion. The reaction mixture was first stirred for 1 h at 0 °C and then overnight at room temperature. After completion of the reaction as indicated by TLC, the reaction mixture was concentrated under reduced pressure. The residue was extracted with EtOAc (2x) and the combined extract was washed successively with saturated aqueous $NaHCO_3$ and sodium chloride (NaCl) solutions, dried

over anhydrous $MgSO_4$ and concentrated in-vacuo affording an oily residue. The crude oil was chromatographed on flash column to yield the desired ether derivative.

4.1.2. General Procedure B (Suzuki-Miyaura Coupling).

A solvent mixture of MeOH (5 ml), toluene (20 ml) and potassium carbonate aqueous solution (2 equiv in 1 ml) were sonicated at room temperature for 30 min and then flushed with nitrogen for 30 min. Bromobenzene derivative (1 equiv), substituted phenylboronic acid (1.25 equiv), and tetrakis(triphenylphosphine) palladium(0) [$Pd(PPh_3)_4$] (0.024 equiv) were added sequentially at room temperature. The reaction mixture was refluxed with stirring under nitrogen atmosphere overnight. The reaction was ceased through stirring in open air for 30 min at room temperature forming a black emulsion. The insoluble material was filtered off through celite pad and the filtrate was extracted with EtOAc (2x). The combined organic phases were washed successively with water, saturated aqueous sodium bicarbonate ($NaHCO_3$), and brine. After drying over anhydrous magnesium sulphate ($MgSO_4$), the solvent was evaporated to dryness in-vacuo affording a brownish yellow sticky mass. The residue was purified by chromatography on silica gel with stepwise gradient elution (*n*-hexane/DCM; 8:2 to 3:7) to give the desired biaryl derivatives.

4.1.3. General procedure C (Knoevenagel Condensation).

To a stirred solution of the appropriate benzaldehyde derivative (1 equiv) in toluene (50 ml) were sequentially added thiazolidine-2,4-dione (**3**; 1 equiv), benzoic acid (0.5 equiv) and piperidine (0.5 equiv). The flask was connected to a Dean-Stark apparatus and a reflux condenser. After refluxing overnight, the reaction mixture is reduced then cooled and placed in the fridge overnight. In case of formed precipitant, the reaction suspension was filtered and the residue was washed with cold water and hexane. The washed residue was dried in oven at 45 °C overnight affording the desired derivatives of the 5-benzylidenethiazolidine-2,4-dione as canary yellow residues. However, in case of absence of precipitant, the reaction mixture

was extracted with EtOAc (2x), washed successively with saturated aqueous $NaHCO_3$ and brine, dried over anhydrous $MgSO_4$, and concentrated in vacuo affording the canary yellow crude residues. In both cases, the residue was used for the next step without further purification or analysis.

4.1.4. General Procedure D (olefin reduction)

To a rapidly stirred mixture of 5-benzylidenethiazolidine-2,4-dione derivatives (Knoevenagel condensation products; 1 equiv) in THF (2ml) and 1 M sodium hydroxide solution (0.06 equiv), was added $CoCl_2$-DMG complex solution (0.6 equiv), made from cobaltus chloride hexahydrate (0.07 g) and dimethylglyoxime (0.75 g) in DMF (15 ml) at room temperature. After stirring for 30 min, sodium borohydride aqueous solution (5.8 equiv) was added and the mixture was stirred at 35-40 °C overnight. The reaction mixture was quenched with water and aqueous HCl at 0 °C and extracted with EtOAc (2x). The combined organic fractions were washed with brine, dried over anhydrous $MgSO_4$ and concentrated under reduced pressure. Purification of the afforded yellowish crude residue by flash column chromatography furnished the desired end products of the three KM Series.

4.1.5. Thiazolidine-2,4-dione (2)

To a solution of chloroacetic acid (5 g, 52.91 mmol) in 6 ml of water was added thiourea (**1**) (4 g, 52.91 mmol) in 6 ml of water. After stirring for 30 min accompanied by considerable cooling, a white precipitant was separated out. The product was filtered, washed with water to remove traces of HCl and finally dried. It was purified by recrystallization in hot water affording the above titled compound as white crystals (5.39 g). Yield: 87%; mp: 125-127 °C; ^{1}H-NMR (300 MHz, DMSO-d_6): δ 4.14 (s, 2H), 12.02 (br s, 1H); MS (EI^+) *m/z*: 117 [M^+].

4.1.6. 5-(4-hydroxybenzylidene)thiazolidine-2,4-dione (3)

Prepared as reported above, by the general procedure C for Knoevenagel condensation, using the commercially available 4-hydroxybenzaldehyde (2 g, 16.38 mmol), the previously prepared **2** (1.9 g, 16.38 mmol), benzoic acid (0.98 g, 8.19 mmol), and piperidine (0.79 ml, 8.19 mmol) in toluene. The precipitant was filtered, washed with cold water, EtOH, and hexane. The above addressed compound was obtained as canary yellow powder (2.72 g). Yield: 75%; mp: > 300 °C; IR (KBr): 3402, 3120, 2998, 2864, 1721, 1677, 1570, 1504, 1332, 1213, 900, 692; ^{1}H-NMR (300 MHz, DMSO-d_6): δ 6.89-6.92 (d, J = 8.67 Hz, 2H), 7.43-7.46 (d, J = 8.67 Hz, 2H), 7.70 (s, 1H), 10.31 (br s, 1H); ^{13}C-NMR (300 MHz, DMSO-d_6): δ 116.31, 118.97, 123.93, 132.29, 132.35, 159.86, 167.48, 168.04; MS (EI$^+$) *m/z*: 211 [M$^+$].

4.1.7. 5-(4-(benzyloxy)benzylidene)thiazolidine-2,4-dione (4)

To a stirred suspension of **3** (0.30 g, 1.36 mmol) and Cs_2CO_3 (0.88 g, 2.71 mmol) in anhydrous DMF (10 ml) was added benzyl chloride (0.19 ml, 1.63 mmol) dropwise. The reaction mixture was stirred at room temperature under nitrogen atmosphere for 4 h. After completion, the reaction mixture was extracted with EtOAc (2x) and the combined organic phases were washed successively with water and brine, and dried over anhydrous $MgSO_4$. The solvent was evaporated to dryness under reduced pressure affording the desired title compound in quantitative yield as yellowish green solid (0.42 g). Yield: 67%; mp: 75-77 °C; IR (Nujol): 1684, 1597, 1506, 1445, 1309, 1152, 1035, 673; ^{1}H-NMR (300 MHz, $CDCl_3$): δ 5.13 (s, 2H), 7.03-7.13 (m, 2H), 7.23-7.31 (m, 2H), 7.34-7.39 (m, 1H), 7.43-7.53 (m, 2H), 7.58-7.66 (m, 1H), 7.80-7.98 (m, 2H), 9.91 (s, 1H); ^{13}C-NMR (300 MHz, $CDCl_3$): δ 69.28, 115.09, 122.79, 125.82, 130.26, 130.33, 131.38, 131.99, 138.26, 163.32, 190.65; MS (EI$^+$) *m/z*: 290 [M$^+$], 292 [M+2] showing relative intensity ratio ~ 1:1.

4.1.8. 5-(4-(benzyloxy)benzyl)thiazolidine-2,4-dione (5)

This compound was accessed in a straightforward fashion from **4** (0.20 g, 0.64 mmol) by means of the general procedure D for reduction except that the reaction time was set for 8 h instead of overnight. Column purification (100% DCM to DCM/MeOH; 97:3, stepwise gradient) furnished the desired reduced end product as a pale yellow solid (0.19 g). Yield: 95%; mp: > 300 °C; ^{1}H-NMR (300 MHz, DMSO-d_6): δ 3.06 (dd, J = 9.03, 14.20 Hz, 1H), 3.33 (dd, J = 4.20, 14.20 Hz, 1H), 4.87 (dd, J = 4.20, 9.03 Hz, 1H), 5.07 (s, 1H), 5.19 (s, 1H), 6.91-6.99 (m, 2H), 7.13-7.20 (m, 2H), 7.26-7.51 (m, 4H), 7.74 (s, 1H), 12.25 (br s, 1H); ^{13}C-NMR (400 MHz, DMSO-d_6): δ 36.76, 53.48, 69.64, 115.12, 116.17, 126.21, 128.20, 128.88, 130.84, 132.52, 136.97, 137.54, 157.90, 168.55, 176.18; MS (ESI$^+$) *m/z*: 336 [M+Na]$^+$.

4.1.9. 4-((3-bromobenzyl)oxy)benzaldehyde (7a)

Mitsunobu coupling of 3-bromobenzyl alcohol (**6a**) (2.30 g, 12.28 mmol) with 4-hydroxybenzaldehyde, (1.5 g, 12.28 mmol) was performed as described in the general procedure B affording yellow oily crude residue. Purification via silica gel column chromatography (*n*-hexane/DCM; 8:2 to 1:9 stepwise gradient) gave the product as a fluffy icy-white solid (2.40 g). Yield: 67%; mp: 75-77 °C; IR (Nujol): 1684, 1597, 1506, 1445, 1309, 1152, 1035, 673; ^{1}H-NMR (300 MHz, $CDCl_3$): δ 5.13 (s, 2H), 7.03-7.13 (m, 2H), 7.23-7.31 (m, 1H), 7.34-7.39 (m, 1H), 7.43-7.53 (m, 1H), 7.58-7.66 (m, 1H), 7.80-7.98 (m, 2H), 9.91 (s, 1H); ^{13}C-NMR (300 MHz, $CDCl_3$): δ 69.28, 115.09, 122.79, 125.82, 130.26, 130.33, 131.38, 131.99, 138.26, 163.32, 190.65; MS (EI$^+$) *m/z*: 290 [M$^+$], 292 [M+2] showing relative intensity ratio ~ 1:1.

4.1.10. 4-((4-bromobenzyl)oxy)benzaldehyde (7b)

Mitsunobu coupling of 4-bromobenzyl alcohol (**6b**) (0.77 g, 4.09 mmol)with 4-hydroxybenzaldehyde (0.5 g, 4.09 mmol), as described in the general procedure B, afforded an orange oily crude residue. Purification via silica gel column chromatography with

stepwise gradient elution (*n*-hexane/DCM; 8:2 to 2:8) gave icy-white crystals (0.83 g). Yield: 70%; mp: 95-97 °C; ^{1}H-NMR (400 MHz, DMSO-d_6): δ 5.12 (s, 2H), 7.08 (d, J = 8.80 Hz, 2H), 7.33 (d, J = 8.31 Hz, 2H), 7.55 (d, J = 8.31 Hz, 2H), 7.86 (d, J = 8.80 Hz, 2H), 9.91 (s, 1H); MS (EI^{+}) *m/z*: 290 [M^{+}], 292 [M+2] showing relative intensity ratio ~ 1:1.

4.1.11. 4-([1,1'-biphenyl]-3-ylmethoxy)benzaldehyde (8a)

Aryl bromide key intermediate **7a (**0.30 g, 1.03 mmol), obtained from the reaction described above, was coupled with phenyl boronic acid (0.16 g, 1.29 mmol) as described in the general procedure B for Suzuki-Miyaura coupling, to give a yellowish white solid (0.19 g). Yield: 63%; mp: 73-75 °C; ^{1}H-NMR (300 MHz, $CDCl_3$): δ 5.23 (s, 2H), 7.12 (d, J = 8.79 Hz, 2H), 7.31-7.55 (m, 5H), 7.55-7.76 (m, 4H), 7.81 (d, J = 8.79 Hz, 2H), 9.91 (s, 1H); ^{13}C-NMR (300 MHz, $CDCl_3$): δ 70.29, 115.14, 126.30, 126.35, 127.17, 127.53, 128.81, 129.18, 130.20, 132.02,136.45, 140.66, 141.83, 163.68, 190.78; MS (EI^{+}) *m/z*: 288 [M^{+}].

4.1.12. 4-((2'-methyl-[1,1'-biphenyl]-3-yl)methoxy)benzaldehyde (8b)

This compound was prepared from **7a** (0.30 g, 1.03 mmol) and o-tolyl boronic acid (0.18 g, 1.29 mmol) using a procedure similar to that used for **8a**, and obtained as an off-white solid (0.23 g). Yield: 75%; mp: 83-85 °C; ^{1}H-NMR (300 MHz, $CDCl_3$): δ 2.26 (s, 3H), 5.22 (s, 2H), 7.04-7.16 (m, 2H), 7.19-7.26 (m, 1H), 7.28-7.37 (m, 2H), 7.39-7.58 (m, 4H), 7.60-7.74 (m, 1H), 7.81-7.92 (m, 2H), 9.90 (s, 1H); ^{13}C-NMR (300 MHz, $CDCl_3$): δ 20.40, 70.22, 115.17, 125.82, 127.47, 128.25, 128.49, 129.14, 129.70, 130.15, 130.36, 131.97, 132.14, 135.26, 135.79, 141.35, 142.44, 163.70, 190.76; MS (EI^{+}) *m/z*: 302 [M^{+}].

4.1.13. 4-((2',6'-dimethyl-[1,1'-biphenyl]-3-yl)methoxy)benzaldehyde (8c)

This compound was prepared from **7a** (0.30 g, 1.03 mmol) and (2,6-dimethyl phenyl)boronic acid (0.19 g, 1.29 mmol) in a manner similar to that used for **8a**, and furnished the end product as a yellowish white oil (0.23 g). Yield: 71%; ^{1}H-NMR (300 MHz,

$CDCl_3$): δ 2.02 (s, 6H), 5.22 (s, 2H), 7.11 (d, J = 9.03 Hz, 2H), 7.14-7.19 (m, 4H), 7.23 (s, 1H), 7.37-7.53 (m, 2H), 7.84 (d, J = 9.03 Hz, 2H), 9.90 (s, 1H); ^{13}C-NMR (300 MHz, $CDCl_3$): δ 20.83, 70.17, 115.22, 125.56, 127.19, 127.32, 127.96, 128.85, 128.95, 130.06, 131.94, 135.94, 136.17, 141.25, 141.52, 163.65, 190.80; MS (EI^+) *m/z*: 316 [M^+].

4.1.14. 4-((4'-(trifluoromethyl)-[1,1'-biphenyl]-3-yl)methoxy)benzaldehyde (8d)

This compound was prepared from **7a** (0.30 g, 1.03 mmol) and (4-(trifluoromethyl)phenyl)boronic acid (0.25 g, 1.29 mmol) using the procedure described for **8a**, and obtained as a thick orange oil (0.29 g). Yield: 79%; mp: 95-96 °C; ^{1}H-NMR (300 MHz, $CDCl_3$): δ 5.24 (s, 2H), 7.12 (d, J = 8.79 Hz, 2H), 7.44-7.64 (m, 3H), 7.64-7.79 (m, 5H), 7.88 (d, J = 8.79 Hz, 2H), 9.92 (s, 1H); ^{13}C-NMR (300 MHz, $CDCl_3$): δ 70.07, 115.11, 125.80, 126.36, 127.22, 127.28, 127.48, 129.42, 130.23, 132.06, 136.78, 140.35, 144.28, 163.57, 190.80; MS (EI^+) *m/z*: 356 [M^+].

4.1.15. 5-(4-([1,1'-biphenyl]-3-ylmethoxy)benzyl)thiazolidine-2,4-dione (1a)

The corresponding Knoevenagel product **9a** (0.15 g, 0.39 mmol), obtained using the general procedure C illustrated above and without further purification, was selectively reduced with $NaBH_4$ (0.09 g, 2.26 mmol) and $CoCl_2$-DMG complex (0.09 ml, 0.24 mmol) as described in the general procedure D. The purification using silica gel column chromatography (100% DCM to DCM/MeOH; 98:2 stepwise gradient) afforded the desired reduced end product in sub-quantitative yield as a pale yellowish white solid (0.12 g). Yield: 81%; mp: >300 °C; ^{1}H-NMR (300 MHz, DMSO-d_6): δ 3.06 (dd, J = 9.03, 13.92 Hz, 1H), 3.29 (dd, J = 4.39, 13.92 Hz, 1H), 4.87 (dd, J = 4.39, 9.03 Hz, 1H), 5.14 (s, 1H), 5.26 (s, 1H), 6.98 (d, J = 8.30 Hz, 2H), 7.14-7.23 (m, 2H), 7.34-7.68 (m, 8H), 7.73-7.77 (m, 1H), 12.22 (br s, 1H); ^{13}C-NMR (300 MHz, $CDCl_3$): δ 36.28, 52.95, 69.12, 114.67, 125.72, 126.00, 126.67,

128.91, 130.33, 137.20, 137.77, 139.82, 140.29, 140.37, 157.40, 167.92, 175.61; MS (ESI^+) *m/z*: 412 $[M+Na]^+$.

4.1.16. 5-(4-((2'-methyl-[1,1'-biphenyl]-3-yl)methoxy)benzyl)thiazolidine-2,4-dione (1b)

Reduction of the corresponding Knoevenagel product **9b (**0.15 g, 0.37 mmol), obtained from the general procedure C, was achieved in a manner similar to that described for **10a**. The title end product was obtained as yellow thick solid (0.09 g). Yield: 61%; mp: 148-150 °C; ^{1}H-NMR (300 MHz, DMSO-d_6): δ 2.02 (s, 3H), 3.07 (dd, J = 9.05, 13.92 Hz, 1H), 3.32 (dd, J = 4.15, 13.92 Hz, 1H), 4.89 (dd, J = 4.15, 9.05 Hz, 1H), 5.14 (s, 1H), 5.26 (s, 1H), 6.92-7.00 (m, 2H), 7.15-7.32 (m, 2H), 7.38-7.66 (m, 7H), 7.72 (s, 1H), 12.19 (br s, 1H); ^{13}C-NMR (300 MHz, $CDCl_3$): δ 20.04, 36.27, 52.96, 69.35, 115.96, 124.84, 125.85, 125.90, 126.16, 128.60, 129.41, 130.30, 134.62, 136.49, 137.04, 140.91, 141.39, 157.35, 171.58, 175.64; MS (EI^+) *m/z*: 403 $[M^+]$.

4.1.17. 5-(4-((2',6'-dimethyl-[1,1'-biphenyl]-3-yl)methoxy)benzyl)thiazolidine-2,4-dione (1c)

Reduction of **9c** (0.15 g, 0.36 mmol), obtained from the general procedure C, was achieved in a similar manner to that described for **10a**. The title product was afforded as yellow thick solid (0.10 g). Yield: 68%; mp: 149-151 °C; ^{1}H-NMR (300 MHz, DMSO-d_6): δ 1.94 (s, 6H), 3.05 (dd, J = 9.03, 13.92 Hz, 1H), 3.33 (dd, J = 4.15, 13.92 Hz, 1H), 4.85 (dd, J = 4.15, 9.03 Hz, 1H), 5.14 (s, 1H), 5.26 (s, 1H), 6.95 (d, J = 8.79 Hz, 2H), 7.08-7.21 (m, 7H), 7.41-7.57 (m, 1H), 7.70 (s, 1H), 12.01 (br s, 1H); ^{13}C-NMR (300 MHz, $CDCl_3$): δ 20.43, 36.79, 52.97, 66.96, 114.78, 124.84, 127.22, 127.92, 130.24, 135.08, 135.10, 136.51, 139.10, 140.39, 141.06, 157.26, 171.59, 175.67; MS (EI^+) *m/z*: 417 $[M^+]$.

4.1.18. 5-(4-((4'-(trifluoromethyl)-[1,1'-biphenyl]-3-yl)methoxy)benzyl) thiazolidine-2,4-dione (1d)

Reduction of the corresponding Knoevenagel product **9d** (0.15 g, 0.33 mmol) was achieved in a procedure similar to that used for **10a**. The title product was afforded as yellowish brown solid (0.10 g). Yield: 69%; mp: >300 °C; ^{1}H-NMR (400 MHz, DMSO-d_6): δ 3.07 (dd, J = 9.05, 14.06 Hz, 1H), 3.30 (dd, J = 4.16, 14.06 Hz, 1H), 4.88 (dd, J = 4.16, 9.05 Hz, 1H), 5.17 (s, 2H), 7.00 (d, J = 8.56 Hz, 2H), 7.15-7.22 (m, 2H), 7.50-7.60 (m, 2H), 7.67-7.76 (m, 1H), 7.83 (d, J = 8.56 Hz, 3H), 7.87-7.96 (m, 2H), 12.09 (br s, 1H); ^{13}C-NMR (400 MHz, $CDCl_3$): δ 36.74, 53.48, 69.48, 115.17, 126.26, 126.30, 126.89, 127.02, 127.22, 128.00, 128.27, 129.39, 129.77, 130.88, 132.55, 138.56, 139.21, 144.40, 157.86, 172.15, 176.18; MS (ESI^+) *m/z*: 457 [M^+].

4.1.19. 5-(4-((3-bromobenzyl)oxy)benzyl)thiazolidine-2,4-dione (11a)

Reduction of the olefin in the corresponding Knoevenagel product **10a** (0.15 g, 0.38 mmol) was achieved according to the general procedure D. The title end product was obtained as yellow solid (0.11 g). Yield: 76%; mp: >300 °C; ^{1}H-NMR (300 MHz, DMSO-d_6): δ 3.06 (dd, J = 9.03, 14.06 Hz, 1H), 3.33 (dd, J = 4.39, 14.06 Hz, 1H), 4.88 (dd, J = 4.39, 9.03 Hz, 1H), 5.09 (s, 2H), 6.92-6.99 (m, 2H), 7.14-7.20 (m, 2H), 7.35 (dd, J = 7.69, 8.79 Hz, 1H), 7.45 (d, J = 7.69 Hz, 1H), 7.53 (d, J = 8.79 Hz, 1H), 7.65 (s, 1H), 11.98 (br s, 1H); ^{13}C-NMR (400 MHz, $CDCl_3$): δ 36.74, 53.45, 69.14, 115.15, 121.39, 129.45, 130.87, 131.82, 131.90, 132.55, 136.47, 137.04, 157.70, 160.31, 172.13, 175.67; MS (ESI^+) *m/z*: 414 [M+Na]$^+$.

4.1.20. 5-(4-((4-bromobenzyl)oxy)benzyl)thiazolidine-2,4-dione (11b)

Reduction of the olefin in the corresponding Knoevenagel product **10b** (0.15 g, 0.38 mmol) was achieved in a manner similar to according to the general procedure D. The title

product was afforded as yellow solid 10.12 g). Yield: 80%; mp: >300 °C; ^{1}H-NMR (400 MHz, DMSO-d_6): δ 3.07 (dd, J = 8.93, 14.06 Hz, 1H), 3.29 (dd, J = 4.28, 14.06 Hz, 1H), 4.88 (dd, J = 4.28, 8.93 Hz, 1H), 5.06 (s, 2H), 6.95 (d, J = 8.56 Hz, 2H), 7.17 (d, J = 8.56 Hz, 2H), 7.39-7.44 (m, 2H), 7.57-7.62 (m, 2H), 12.02 (br s, 1H); ^{13}C-NMR (400 MHz, $CDCl_3$): δ 36.74, 53.45, 68.82, 115.15, 121.39, 129.45, 130.29, 131.82, 131.90, 132.55, 136.47, 137.04, 157.70, 172.13, 175.16; MS (ESI^+) *m/z*: 414 $[M+Na]^+$.

4.1.21. (*R*)-(+)-3-chloro-1-phenyl-propan-1-ol (13)

Step 1: a flask was charged with (*S*)-(–)-α,α-diphenylprolinol (0.30 g, 1.19 mmol) and anhydrous toluene (7 ml). The mixture was placed under nitrogen by evacuation and filling three times. The borane tetrahydrofuran complex solution **[**BH_3•THF; 1 M solution in THF, stabilized with 5 mM $NaBH_4$] (0.35 ml, 3.56 mmol) was added in a dropwise fashion at 30 °C and the clear solution was stirred for 30 min. Step 2: to this stirred solution, 3-chloro-1-phenylpropan-1-one **12** (1 g, 5.93 mmol) in anhydrous toluene (1 ml) was added. The reaction mixture was then stirred at room temperature for 15 min followed by the addition of BH_3•THF (6 ml, 61.44 mmol) over a period of 3 min. After stirring for additional 90 min, the reaction flask was cooled in ice bath and quenched successively with MeOH (10 ml), isopropanole (10 ml), and HCl (3 ml), and was passed through a pad of Celite. The filtrate was concentrated to dryness and crystallized from hexane. The title compound was obtained as white fluffy solid (4.91 g). Yield: 97%; m.p. 57-59 ℃; $[\alpha]^{25}_{D}$ = + 25.7 ° (c 1, $CHCl_3$); ^{1}H-NMR (400 MHz, $CDCl_3$): δ 2.07-2.16 (m, 2H), 2.20-2.32 (m, 1H), 3.51-3.62 (m, 1H), 3.71-3.80 (m, 1H), 4.91-4.98 (m, 1H), 7.37-7.43 (m, 5H), ^{13}C-NMR (400 MHz, $CDCl_3$): δ 41.45, 41.73, 71.34, 125.80, 127.94, 128.69, 143.71; MS (EI^+) *m/z*: 170 $[M^+]$, 172 [M+2] showing relative intensity ratio ~ 3:1.

4.1.22. (*R*)-4-(3-hydroxy-3-phenylpropoxy)benzaldehyde (14)

After nitrogen substitution, 4-hydroxybenzaldehyde (2.15 g, 17.58 mmol) was dissolved in a mixture of anhydrous THF/DMF (2:1v/v, 15 ml), and Cs_2CO_3 (5.73 g, 17.58 mmol) was added at room temperature. The mixture was stirred at 50 °C in a water bath for 1 h. Compound **13** (1 g, 5.86 mmol) was added and the system was stirred at 50 °C overnight. The reaction mixture was cooled, diluted with EtOAc (2x) and washed successively with saturated aqueous $NaHCO_3$ and brine. The combined organic layer was washed then with 1 M aqueous NaOH (3 x 25 ml) in order to remove the excess 4-hydroxybenzaldehyde. Finally, the mixture was dried over MgSO4 and evaporated to dryness affording the title key intermediate as a thick yellow oil (2.26 g). Yield: 95 %; $[\alpha]^{25}_{D} = -3.7$ ° (*c* 2.3, $CHCl_3$); ^{1}H-NMR (300 MHz, $CDCl_3$): δ 2.19-2.38 (m, 2H), 2.99 (br s, 1H), 4.13 (dt, *J* = 5.37, 9.52 Hz, 1H), 4.28 (ddd, *J* = 5.37, 7.08, 9.52 Hz, 1H), 5.02 (dd, *J* = 5.37, 7.08 Hz, 1H), 6.94-7.08 (m, 2H), 7.29-7.47 (m, 5H), 7.79-7.90 (m, 2H), 9.89 (s, 1H); ^{13}C-NMR (400 MHz, $CDCl_3$): δ 37.14, 64.38, 70.34, 113.78, 124.73, 126.78, 127.59, 128.91, 131.01, 142.99, 162.88, 189.92 ; MS (EI^+) *m/z*: 256 [M^+].

4.1.23. (*S*)-4-(3-phenoxy-3-phenylpropoxy)benzaldehyde (15a)

Starting from **14** (0.50 g, 1.95 mmol) and phenol (0.18 g, 1.95 mmol), the steps of the general procedure A described above for Mitsunobu coupling provided the title compound. After flash column purification (*n*-hexane/EtOAc; 95:5 to 7:3 stepwise gradient), the target compound was obtained as a colorless oil solidified in the fridge (0.38 g). Yield: 59%; ^{1}H-NMR (300 MHz, $CDCl_3$): δ 2.24-2.42 (m, 1H), 2.42-2.60 (m, 1H), 4.14 (dt, *J* = 4.43, 9.42 Hz, 1H), 4.33 (ddd, *J* = 4.43, 8.06, 9.42 Hz, 1H), 5.42 (dd, *J* = 4.43, 8.06 Hz, 1H), 6.81-6.92 (m, 3H), 7.00 (d, *J* = 8.06 Hz, 2H), 7.26-7.47 (m, 7H), 7.83 (d, *J* = 8.06 Hz, 2H), 9.89 (s, 1H); MS (EI^+) *m/z*: 332 [M^+].

4.1.24. (*S*)-4-(3-phenyl-3-(m-tolyloxy)propoxy)benzaldehyde (15b)

The title compound was prepared from **14** (0.50 g, 1.95 mmol) and m-cresol (0.21 g, 1.95 mmol) using the same method as **15a** giving a thick yellow oil which solidifies in the fridge (0.43 g). Yield: 63%; ^{1}H-NMR (300 MHz, $CDCl_3$): δ 2.25 (s, 3H), 2.28-2.38 (m, 1H), 2.41-2.54 (m, 1H), 4.06-4.19 (dt, *J* = 4.83, 9.39 Hz, 1H), 4.25-4.37 (m, 1H), 5.41 (dd, *J* = 4.83, 8.46 Hz, 1H), 6.60-6.72 (m, 4H), 6.95-7.07 (m, 3H), 7.33-7.40 (m, 4H), 7.83 (d, *J* = 8.86 Hz, 2H), 9.89 (s, 1H); MS (EI^+) *m/z*: 346 [M^+].

4.1.25. (*S*)-4-(3-phenyl-3-(p-tolyloxy)propoxy)benzaldehyde (15c)

The title compound was prepared from **14** (0.50 g, 1.95 mmol) and p-cresol (0.21 g, 1.95 mmol), in a manner similar to that described for **15a**, as yellow thick oil which solidifies in the fridge (0.38 g). Yield: 56%; ^{1}H-NMR (300 MHz, $CDCl_3$): δ 2.22 (s, 3H), 2.31-2.56 (m, 2H), 4.13 (dt, *J* = 4.64, 7.55 Hz, 1H), 4.25-4.40 (m, 1H), 5.37 (dd, *J* = 4.64, 8.75 Hz, 1H), 6.68-6.79 (m, 2H), 6.93-7.07 (m, 4H), 7.28-7.47 (m, 5H), 7.75-7.93 (m, 2H), 9.89 (s, 1H); ^{13}C-NMR (400 MHz, $CDCl_3$): δ 19.38, 37.12, 63.66, 70.24, 113.79, 114.79, 124.88, 126.71, 127.70, 128.78, 130.96, 140.32, 154.78, 162.88, 189.79; MS (EI^+) *m/z*: 346 [M^+].

4.1.26. (*S*)-4-(3-(3-methoxyphenoxy)-3-phenylpropoxy)benzaldehyde (15d)

The title compound was prepared from **14** (0.50 g, 1.95 mmol) and 3-methoxyphenol (0.24 g, 1.95 mmol), in a manner similar to that described for **15a**, as a thick colorless oil which solidifies in the fridge (0.29 g). Yield: 41%; ^{1}H-NMR (300 MHz, $CDCl_3$): δ 2.22-2.41 (m, 1H), 2.41-2.57 (m, 1H), 3.67-3.75 (s, 3H), 4.04-4.17 (m, 1H), 4.30 (dd, *J* = 5.54, 9.75 Hz, 1H), 5.40 (dd, *J* = 5.54, 7.55 Hz, 1H), 6.39-6.50 (m, 4H), 6.95-7.08 (m, 3H), 7.33-7.42 (m, 4H), 7.77-7.87 (m, 2H), 9.88 (s, 1H); MS (EI^+) *m/z*: [M^+].

4.1.27. (*S*)-4-(3-phenyl-3-(4-(trifluoromethyl)phenoxy)propoxy)benzaldehyde (15e)

The title compound was prepared from **14** (0.50 g, 1.95 mmol) and 4-(trifluoromethyl) phenol (0.32 g, 1.95 mmol), in a manner similar to that described for **15a**, as a thick yellow

thick oil (0.35 g). Yield: 45%; ^{1}H-NMR (300 MHz, $CDCl_3$): δ 2.18-2.44 (m, 2H), 4.12 (dt, *J* = 4.73, 7.05 Hz, 1H), 4.22-4.39 (m, 1H), 5.48 (dd, *J* = 4.73, 8.36 Hz, 1H), 6.92 (d, *J* = 8.26 Hz, 2H), 7.00 (d, *J* = 8.26 Hz, 2H), 7.34-7.46 (m, 7H), 7.76-7.87 (m, 2H), 9.88 (s, 1H); MS (EI^+) *m/z*: [M^+].

4.1.28. (*S*)-4-(3-(4-chlorophenoxy)-3-phenylpropoxy)benzaldehyde (15f)

The title compound was prepared from **14** (0.50 g, 1.95 mmol) and 4-chlorophenol (0.25 g, 1.95 mmol), in a manner similar to that described for **15a**, as a yellow oil (0.44 g). Yield: 61%; ^{1}H-NMR (300 MHz, $CDCl_3$): δ 2.29-2.39 (m, 1H), 2.41-2.59 (m, 1H), 4.11 (dt, *J* = 5.24, 7.25 Hz, 1H), 4.23-4.37 (m, 1H), 5.37 (dd, *J* = 5.24, 8.16 Hz, 1H), 6.78 (dd, *J* = 1.71, 8.96 Hz, 2H), 7.00 (dd, *J* = 1.71, 8.96 Hz, 2H), 7.09-7.16 (m, 2H), 7.34-7.44 (m, 5H), 7.83 (dd, *J* = 1.41, 8.76 Hz, 2H), 9.89 (d, *J* = 1.41 Hz, 1H); MS (EI^+) *m/z*:366 [M^+], 368 [M+2] showing relative intensity ratio ~ 3:1.

4.1.29. (*S*)-4-(3-(2,4-dichlorophenoxy)-3-phenylpropoxy)benzaldehyde (15g)

The title compound was prepared from **14** (0.50 g, 1.95 mmol) and 2,4-dichlorophenol (0.32 g, 1.95 mmol), in a manner similar to that described for **15a**, as a thick yellow oil (0.33 g). Yield: 42%; ^{1}H-NMR (300 MHz, $CDCl_3$): δ 2.29-2.32 (m, 1H), 2.36-2.43 (m, 1H), 4.09 (dt, *J* = 4.33, 8.16 Hz, 1H), 4.96 (m, 1H), 5.42 (dd, *J* = 4.33, 7.57 Hz, 1H), 6.64 (d, *J* = 9.06 Hz, 2H), 6.91-7.04 (m, 2H), 7.33-7.41 (m, 6H), 7.78-7.87 (m, 2H), 9.89 (s, 1H); MS (EI^+) *m/z*: 400 [M^+], 402 [M+2], 404 [M+4] showing relative intensity ratio 9:6:1.

4.1.30. 5-(4-((*S*)-3-phenoxy-3-phenylpropoxy)benzyl)thiazolidine-2,4-dione (2a)

The corresponding Knoevenagel product **16a** (0.20 g, 0.46 mmol), obtained using the general procedure C without further purification, was reduced with $NaBH_4$ (0.10 g, 2.67 mmol) and $CoCl_2$-DMG complex (0.10 ml, 0.28 mmol) as described in the general procedure D. Purification using silica gel column chromatography (100 % DCM to DCM/MeOH; 98:2

stepwise gradient) afforded the desired reduced end product as yellow sticky solid (0.19 g). Yield: 94%; mp: 90-92 °C; ^{1}H-NMR (400 MHz, $CDCl_3$): δ 2.13-2.30 (m, 1H), 2.34-2.47 (m, 1H), 3.01 (dd, *J* = 9.41, 14.31 Hz, 1H), 3.38 (dd, *J* = 3.91, 14.31 Hz, 1H), 4.02 (dt, *J* = 4.65, 9.57 Hz, 1H), 4.09-4.16 (m, 1H), 4.42 (dd, *J* = 3.91, 9.41 Hz, 1H), 5.33 (dd, *J* = 4.65, 8.31 Hz, 1H), 6.73 - 6.82 (m, 3H), 6.90 (d, *J* = 8.56 Hz, 1H), 7.01 - 7.13 (m, 2H), 7.14 - 7.23 (m, 2H), 7.23 - 7.42 (m, 5H), 7.74 (s, 1H), 8.88 (br s, 1H); ^{13}C-NMR (400 MHz, $CDCl_3$): δ 37.82, 38.22, 53.79, 64.58, 76.53, 115.39, 121.00, 125.92, 128.78, 129.38, 130.31, 141.22, 157.96, 158.38, 170.45, 174.20; MS (ESI^+) *m/z*: 456 $[M+Na]^+$.

4.1.31. 5-(4-((*S*)-3-phenyl-3-(m-tolyloxy)propoxy)benzyl)thiazolidine-2,4-dione (2b)

Reduction of the corresponding Knoevenagel product **16b** (0.20 g, 0.45 mmol) was achieved in a manner similar to that described for **2a**. The title end product was obtained as a yellow gummy solid (0.17 g). Yield: 83 %; mp: 110-112 °C; ^{1}H-NMR (400 MHz, $CDCl_3$): δ 2.11-2.17 (m, 3H), 2.18-2.28 (m, 1H), 2.32-2.45 (m, 1H), 3.01 (dd, *J* = 9.33, 14.57 Hz, 1H), 3.38 (dd, *J* = 3.91, 14.57 Hz, 1H), 3.99-4.04 (m, 1H), 4.18-4.23 (m, 1H), 4.42 (dd, *J* = 3.91, 9.33 Hz, 1H), 5.32 (dd, *J* = 4.65, 8.31 Hz, 1H), 6.51-6.65 (m, 3H), 6.77 (d, *J* = 8.56 Hz, 1H), 6.86-6.99 (m, 3H), 7.05 (d, *J* = 8.56 Hz, 1H), 7.15-7.22 (m, 1H), 7.26-7.32 (m, 2H), 7.34-7.37 (m, 1H), 7.73 (s, 1H), 8.88 (br s, 1H); ^{13}C-NMR (400 MHz, $CDCl_3$): δ 25.62, 38.23, 38.41, 53.82, 67.95, 76.40, 115.38, 116.91, 121.86, 125.89, 128.74, 129.09, 132.38, 139.43, 141.36, 157.99, 160.98, 170.59, 174.33; MS (ESI^+) *m/z*: 470 $[M+Na]^+$.

4.1.32. 5-(4-((*S*)-3-phenyl-3-(p-tolyloxy)propoxy)benzyl)thiazolidine-2,4-dione (2c)

Reduction of the corresponding Knoevenagel product **16c** (0.20 g, 0.45 mmol) was achieved in a manner similar to that described for **2a**. The title end product was afforded as a pale yellow gummy solid (0.19 g). Yield: 94 %; mp: 143-145 °C; ^{1}H-NMR (400 MHz, $CDCl_3$): δ 2.13 (s, 3H), 2.18-2.27 (m, 1H), 2.33-2.44 (m, 1H), 3.02 (dd, *J* = 9.23, 14.44 Hz,

1H), 3.39 (dd, *J* = 3.87, 14.44 Hz, 1H), 3.97-4.06 (m, 1H), 4.16-4.27 (m, 1H), 4.41 (dd, *J* = 3.87, 9.23 Hz, 1H), 5.28 (dd, *J* = 4.65, 8.56 Hz, 1H), 6.67 (d, *J* = 8.31 Hz, 2H), 6.77 (d, *J* = 8.56 Hz, 1H), 6.86-6.93 (m, 4H), 7.05 (d, *J* = 8.31 Hz, 2H), 7.17 - 7.37 (m, 4H), 8.96 (br s, 1H); ^{13}C-NMR (400 MHz, $CDCl_3$): δ 25.62, 37.84, 38.21, 53.81, 67.95, 76.69, 115.84, 119.22, 125.93, 128.74, 129.83, 130.26, 132.39, 141.40, 155.92, 158.40, 170.49, 174.24; MS (ESI^+) *m/z*: 470 $[M+Na]^+$.

4.1.33. 5-(4-(3-((*S*)-3-methoxyphenoxy)-3-phenylpropoxy)benzyl)thiazolidine-2,4-dione (2d)

The title compound was obtained via reduction of the corresponding Knoevenagel product **16d** (0.20 g, 0.43 mmol) in a manner similar to that described for **2a**. The product was afforded as a yellow sticky solid (0.15 g). Yield: 76 %; mp: 161-163 °C; ^{1}H-NMR (400 MHz, $CDCl_3$): δ 2.12-2.29 (m, 1H), 2.38 (dddd, *J* = 2.81, 5.62, 8.50, 11.43 Hz, 1H), 3.00 (dd, *J* = 9.87, 14.18 Hz, 1H), 3.37 (dd, *J* = 3.79, 14.18 Hz, 1H), 3.59 (s, 3H), 3.95-4.04 (m, 1H), 4.15-4.25 (m, 1H), 4.40 (dd, *J* = 3.79, 9.87 Hz, 1H), 5.32 (dd, *J* = 5.62, 8.50 Hz, 1H) 6.31-6.41 (m, 3H), 6.71-6.80 (m, 1H), 6.87-7.07 (m, 3H), 7.14-7.22 (m, 1H), 7.25-7.33 (m, 4H), 7.36 (d, *J* = 8.80 Hz, 1H), 8.91 (br s, 1H); ^{13}C-NMR (400 MHz, $CDCl_3$): δ 25.62, 36.99, 38.16, 55.20, 64.55, 76.62, 102.49, 106.42, 108.24, 115.38, 119.31, 125.88, 127.84, 128.80, 129.79, 132.38, 141.18, 159.20, 160.66, 166.91, 167.45; MS (ESI^+) *m/z*: 486 $[M+Na]^+$.

4.1.34. 5-(4-((*S*)-3-phenyl-3-(4-(trifluoromethyl)phenoxy)propoxy)benzyl) thiazolidine-2,4-dione (2e)

The title compound was obtained via reduction of the corresponding Knoevenagel product **16e** (0.20 g, 0.40 mmol) in a manner similar to that described for **2a**. The product was obtained as a yellow sticky solid (0.13 g). Yield: 64%; mp: 120-122 °C; ^{1}H-NMR (400 MHz, $CDCl_3$): δ 2.20-2.32 (m, 1H), 2.35-2.49 (m, 1H), 3.01 (dd, *J* = 9.75, 14.25 Hz, 1H), 3.38 (dd,

J = 4.00, 14.25 Hz, 1H), 4.00 (dt, *J* = 5.59, 9.60 Hz, 1H), 4.17-4.23 (m, 1H), 4.41 (dd, *J* = 4.00, 9.75 Hz, 1H), 5.39 (dd, *J* = 5.59, 8.19 Hz, 1H), 6.76 (d, *J* = 8.56 Hz, 1H), 6.80-6.86 (m, 2H), 6.88-6.95 (m, 1H), 7.05 (d, *J* = 8.56 Hz, 1H), 7.16-7.31 (m, 5H), 7.33-7.40 (m, 3H), 9.07 (br s, 1H); ^{13}C-NMR (400 MHz, $CDCl_3$): δ 30.34, 38.09, 57.77, 64.31,76.83, 115.80, 119.46, 125.84, 126.80, 128.17, 128.97, 132.37, 134.16, 140.29, 160.34, 160.79, 166.77, 167.31; MS (ESI^+) *m/z*: 524 $[M+Na]^+$.

4.1.35. 5-(4-((*S*)-3-(4-chlorophenoxy)-3-phenylpropoxy)benzyl)thiazolidine-2,4-dione (2f)

The title compound was obtained via reduction of the corresponding Knoevenagel product **16f** (0.20 g, 0.43 mmol) in a manner similar to that described for **2a**. The title end product was obtained as a yellow gummy solid (0.12 g). Yield: 60%; mp: 63-65 °C; ^{1}H-NMR (400 MHz, $CDCl_3$): δ 2.22-2.37 (m, 1H), 2.43-2.55 (m, 1H), 3.12 (dd, *J* = 9.66, 14.31 Hz, 1H), 3.47 (dd, *J* = 3.91, 14.31 Hz, 1H), 3.98-4.03 (m, 1H), 4.20 (ddd, J = 4.89, 8.56, 9.54 Hz, 1H), 4.51 (dd, *J* = 3.91, 9.66 Hz, 1H), 5.38 (dd, *J* = 4.89, 8.56 Hz, 1H), 6.79 (d, *J* = 8.60 Hz, 2H), 6.86 (d, *J* = 8.60 Hz, 2H), 7.00 (d, *J* = 8.80 Hz, 1H), 7.14 (m, 2H), 7.33 (m, 5H), 7.46 (d, *J* = 8.80 Hz, 1H), 8.69 (br s, 1H); ^{13}C-NMR (400 MHz, $CDCl_3$): δ 37.82, 38.29, 53.75, 67.95, 77.14, 114.88, 117.31, 125.95, 127.92, 128.87, 129.21, 130.35, 132.37, 140.88, 156.61, 158.30, 170.37, 174.14; MS (ESI^+) *m/z*: 490 $[M+Na]^+$.

4.1.36. 5-(4-((*S*)-3-(2,4-dichlorophenoxy)-3-phenylpropoxy)benzyl)thiazolidine-2,4-dione (2g)

Reduction of the corresponding Knoevenagel product **16g** (0.20 g, 0.40 mmol) was performed in a manner similar to that described for **2a**. The title end product was obtained as a pale yellow solid (0.09 g). Yield: 47%; mp: 71-72 °C; ^{1}H-NMR (400 MHz, $CDCl_3$): δ 2.22-2.31 (m, 1H), 2.37-2.51 (m, 1H), 3.00 (dd, *J* = 9.66, 14.06 Hz, 1H), 3.38 (dd, *J* = 3.91, 14.06

Hz, 1H), 3.90-3.99 (m, 1H), 4.19 (td, *J* = 4.89, 8.68 Hz, 1H), 4.40 (dd, *J* = 3.91, 9.66 Hz, 1H), 5.34 (dd, *J* = 4.89, 8.88 Hz, 1H), 6.52-6.61 (m, 1H), 6.77 (d, *J* = 8.56 Hz, 1H), 6.84-6.94 (m, 2H), 7.05 (d, *J* = 8.56 Hz, 1H), 7.16-7.26 (m, 2H), 7.26-7.32 (m, 4H), 7.36 (d, *J* = 8.80 Hz, 1H), 8.81 (br s, 1H); ^{13}C-NMR (400 MHz, $CDCl_3$): δ 3034, 38.07, 53.75, 67.96, 78.21, 115.35, 119.46, 125.87, 127.38, 128.96, 129.96, 132.36, 134.11, 140.08, 158.26, 160.82, 166.79, 167.39; MS (ESI^+) *m/z*: 501 [M^+].

4.1.37. (1*H*-benzo[*d*]imidazol-2-yl)methanol (18)

To a well stirred mixture of 1,2-phenylenediamine **17** (1 g, 9.25 mmol) in 6 M HCl (10 ml) was added 67% w/v glycolic acid (6.30 ml, 55.48 mmol) dropwise, till the suspension was clear. After stirring for 10 min at room temperature, the reaction flask was plugged to a condenser and refluxed overnight. Reaction mixture was cooled and concentrated under overnight ventilation affording the HCl salt of the title compound as needle crystals. The crystals were washed with least amount of cold EtOH on a filter paper and dried in oven at 45 °C overnight. The dried crystals were dissolven in water and then precipitated with 1 M K_2CO_3 (20 ml) furnishing the title compound as a free base in crude mixture. After the effervescence was settled, the crude residue was extracted with EtOAc (2x), washed with brine and the organic solvent was removed in-vacuo. The pure free base was obtained as white crystals (4.45 g). Yield: 65%; mp: 165-167 °C; IR (KBr): 3257, 3061, 2931, 1617, 1485, 1440, 1347, 1270, 1048, 876, 746, 681; ^{1}H-NMR (300 MHz, DMSO-d_6): δ 4.68 (d, *J* = 5.74 Hz, 2H), 5.63 (t, J = 5.74 Hz, 1H), 7.05-7.22 (m, 2H), 7.48 (dd, *J* = 3.42, 5.86 Hz, 2H), 12.26 (br s, 1H); MS (EI^+) *m/z*: 148 [M^+].

4.1.38. (1-benzyl-1*H*-benzo[*d*]imidazol-2-yl)methanol (19a)

To an ice-bath cooled solution of **18** (0.50 g, 3.38 mmol) in anhydrous DMF (7 ml) was added sodium hydride (NaH; 0.08 g, 3.38 mmol). After stirring at 0 °C for approx. 15 min (or

after no more visible emergence of hydrogen), the mixture was allowed to warm up to room temperature and kept stirred for an additional 45 min. The mixture was then re-cooled to 0 °C, and benzyl chloride (0.39 ml, 3.38 mmol) was slowly added. The mixture was first stirred 1 h at 0 C and then overnight at room temperature. The mixture was then quenched with cold water and crushed ice and extracted with DCM (2x). The combined organic layer was washed with brine, dried over MgSO4 and concentrated under reduced pressure. The residue was purified by silica gel chromatography (100% DCM to DCM/MeOH; 97:3 stepwise gradient) to give the title compound as a yellow sticky solid (0.62 g). Yield: 77 %; mp: 157-159 °C; IR (Nujol): 3142, 2920, 2852, 1606, 1416, 1463, 1344, 1214, 1043, 856, 734; ^{1}H-NMR (300 MHz, $CDCl_3$): δ 4.88 (s, 2H), 5.46 (s, 2H), 7.00-7.16 (m, 2H), 7.16-7.41 (m, 6H), 7.71 (d, 1H); MS (EI^+) *m/z*: 238 [M^+].

4.1.39. (1-isobutyl-1*H*-benzo[*d*]imidazol-2-yl)methanol (19b)

N-Alkylation of **18** (0.50 g, 3.38 mmol) with isobutyl bromide (0.37 ml, 3.38 mmol) was accomplished by the method described above for the synthesis of **19a**. The title compound was obtained as a white solid (0.49 g). Yield: 71%; mp: 105-107 °C; IR (KBr): 3130, 2960, 2860, 1605, 1520, 1463, 1335, 1286, 1054, 891, 741; ^{1}H-NMR (300 MHz, $CDCl_3$): δ 0.95 (d, J = 6.84 Hz, 6H), 2.22-2.34 (m, 1H), 4.02 (d, J = 7.57 Hz, 2H), 4.89 (s, 2H), 7.18-7.33 (m, 3H), 7.64-7.73 (m, 1H); ^{13}C-NMR (300 MHz, $CDCl_3$): δ 20.22, 29.13, 51.23, 56.73, 110.20, 119.12, 122.25, 122.83, 135.35, 139.02, 141.22, 154.07; MS (EI^+) *m/z*: 204 [M^+].

4.1.40. (1-allyl-1*H*-benzo[*d*]imidazol-2-yl)methanol (19c)

N-Alkylation of **18** (0.50 g, 3.38 mmol) with allyl bromide (0.29 ml, 3.38 mmol) was performed by the method described above for the synthesis of **19a**. The title compound was afforded as a yellow sticky solid (0.52 g). Yield: 82%; mp: 88-90 °C; ^{1}H-NMR (300 MHz, $CDCl_3$): δ 2.89 (s, 1H), 2.96 (s, 1H), 4.88 (s, 2H), 5.03 (dd, J = 0.90, 10.40 Hz, 1H), 5.22 (dd,

J = 0.90, 10.40 Hz, 1H), 5.91-6.05 (m, 1H), 7.24-7.31 (m, 3H), 7.66-7.77 (m, 1H); MS (EI^+) *m/z*: 188 [M^+].

4.1.41. (1-isopropyl-1*H*-benzo[*d*]imidazol-2-yl)methanol (19d)

N-Alkylation of **18** (0.50 g, 3.38 mmol) with isopropyl bromide (0.32 ml, 3.38 mmol) was effected by the method described above for the preparation of **19a**. Except, the reaction mixture was stirred at 40 °C for 48 h instead of room temperature overnight. The title compound was afforded as a yellow oil (0.34 g). Yield: 53%; ^{1}H-NMR (400 MHz, $CDCl_3$): δ 2.01-2.35 (m, 6H), 4.93 (br s, 1H), 5.05-5.13 (m, 1H), 5.52 (s, 2H), 7.27-7.39 (m, 1H), 7.43-7.51 (m, 1H), 7.69-7.91 (m, 2H); MS (EI^+) *m/z*: 190 [M^+].

4.1.42. (1-cyclopentyl-1*H*-benzo[*d*]imidazol-2-yl)methanol (19e)

N-Alkylation of **18** (0.50 g, 3.38 mmol) with cyclopentyl bromide (0.36 ml, 3.38 mmol) was accomplished using the method described above for the synthesis of **19a**. Except, the reaction mixture was stirred at 40 °C for 48 h instead of room temperature overnight. The title compound was obtained as a pale yellow oil (0.49 g). Yield: 67%; ^{1}H-NMR (400 MHz, $CDCl_3$): δ 1.14-1.37 (m, 2H), 1.74-1.92 (m, 1H), 2.00-2.11 (m, 2H), 2.11-2.21 (m, 1H), 2.21-2.33 (m, 2H), 4.94 (br s, 1H), 5.03-5.11 (m, 1H), 5.51 (s, 2H), 7.27-7.33 (m, 1H), 7.45-7.53 (m, 1H), 7.72-7.96 (m, 2H); MS (EI^+) *m/z*: 216 [M^+].

4.1.43. 4-((1-benzyl-1*H*-benzo[*d*]imidazol-2-yl)methoxy)benzaldehyde (20a)

This compound was prepared from **19a** (0.4 g, 1.96 mmol) and the commercially available 4-hydroxybenzaldehyde (0.24 g, 1.96 mmol) by means of the general procedure A. The crude oil was chromatographed on flash column with stepwise gradient elution (*n*-hexane/EtOAc; 95:5 to 2:8) to afford the title compound as a thick yellow oil (0.51 g). Yield: 89%; mp: 164-166 °C; ^{1}H-NMR (300 MHz, $CDCl_3$): δ 5.42 (s, 2H), 5.52 (s, 2H), 7.02-7.11 (m, 4H), 7.27-7.37 (m, 6H), 7.70-7.93 (m, 3H), 9.88 (s, 1H); MS (EI^+) *m/z*: 342 [M^+].

4.1.44. 4-((1-isobutyl-1*H*-benzo[*d*]imidazol-2-yl)methoxy)benzaldehyde (20b)

This compound was prepared from **19b** (0.4 g, 1.68 mmol) following the same procedure used for the preparation of **20a**. The crude oil was chromatographed on flash column with stepwise gradient elution (*n*-hexane/EtOAc; 95:5 to 2:8) to afford the title compound as a yellowish white solid (0.53 g). Yield: 87%; mp: 89-91 °C; ^{1}H-NMR (300 MHz, $CDCl_3$): δ 0.98 (d, J = 6.91 Hz, 6H), 2.27-2.42 (m, 1H), 4.10 (d, J = 7.57 Hz, 2H), 5.48 (s, 2H), 7.22-7.41 (m, 5H), 7.78-7.88 (m, 3H), 9.89 (s, 1H); MS (EI^+) *m/z*: 308 [M^+].

4.1.45. 4-((1-allyl-1*H*-benzo[*d*]imidazol-2-yl)methoxy)benzaldehyde (20c)

Using **19c** (0.4 g, 2.13 mmol) and following the procedure used for the preparation of **20a**, gave the title compound as a yellow oil that gradually solidifies in fridge (0.57 g). Yield: 92%; ^{1}H-NMR (400 MHz, $CDCl_3$): δ 4.93 (dd, J = 3.42, 1.47 Hz, 2H), 4.98-5.08 (m, 1H), 5.17-5.26 (m, 1H), 5.41-5.52 (m, 2H), 5.88-6.00 (m, 1H), 7.22 (dd, J = 8.68, 1.59 Hz, 2H), 7.27-7.41 (m, 3H), 7.78-7.89 (m, 3H), 9.88 (d, J = 1.96 Hz, 1H); ^{13}C-NMR (400 MHz, $CDCl_3$): δ 46.51, 63.41, 110.13, 115.22, 117.89, 120.20, 122.73, 123.70, 130.73, 131.68, 132.03, 135.43, 148.22, 162.68, 190.70; MS (EI^+) *m/z*: 292 [M^+].

4.1.46. 4-((1-isopropyl-1*H*-benzo[*d*]imidazol-2-yl)methoxy)benzaldehyde (20d)

Using **19d** (0.4 g, 2.10 mmol) and following the procedure used for the preparation of **20a**, gave the title compound as a thick yellow oil (0.45 g). Yield: 73%; ^{1}H-NMR (400 MHz, $CDCl_3$): δ 1.59 (d, J = 6.85 Hz, 6H), 4.83-4.88 (m, 1H), 5.41 (s, 2H), 7.14 (d, J = 8.56 Hz, 2H), 7.17-7.24 (m, 2H), 7.46-7.53 (m, 1H), 7.70-7.78 (m, 3H), 9.80 (s, 1H); MS (EI^+) *m/z*: 294 [M^+].

4.1.47. 4-((1-cyclopentyl-1*H*-benzo[*d*]imidazol-2-yl)methoxy)benzaldehyde (20e)

This compound was prepared from **19e** (0.4 g, 1.85 mmol) following the procedure used for the preparation of **20a**. The title compound was obtained as a pale yellow oil that

gradually solidifies in fridge (0.46 g). Yield: 77%; ^{1}H-NMR (300 MHz, $CDCl_3$): δ 1.18-1.35 (m, 6H), 2.07-2.12 (m, 2H), 4.09-4.15 (m, 1H), 5.45 (s, 2H), 7.12-7.31 (m, 5H), 7.88-7.98 (m, 3H), 9.89 (s, 1H); MS (EI^+) *m/z*: 320 [M^+].

4.1.48. 5-(4-((1-benzyl-1*H*-benzo[*d*]imidazol-2-yl)methoxy)benzyl)thiazolidine-2,4-dione (5a)

The respective Knoevenagel product **21a** (0.25 g, 0.57 mmol) was selectively reduced with $NaBH_4$ according to the general procedure D. The title end product was afforded as a yellowish white solid (0.22 g). Yield: 87%; mp: 186-188 °C; ^{1}H-NMR (300 MHz, DMSO-d_6): δ 3.07(dd, *J* = 9.03, 14.16 Hz, 1H), 3.31 (dd, *J* = 4.15, 14.16 Hz, 1H), 4.89 (dd, *J* = 4.15, 9.03 Hz, 1H), 5.39 (s, 2H), 5.55-5.71 (m, 2H), 6.86-7.02 (m, 2H), 7.06-7.19 (m, 3H), 7.21-7.31 (m, 5H), 7.42-7.62 (m, 2H), 7.64-7.84 (m, 1H), 11.38 (br s, 1H); ^{13}C-NMR (300 MHz, DMSO-d_6): δ 36.26, 46.84, 52.83, 62.49, 110.64, 114.41, 119.27, 121.78, 122.74, 126.54, 128.30, 130.07, 131.63, 136.40, 141.69, 149.31, 156.49, 171.27, 175.31; MS (ESI^+) *m/z*: 444 $[M+H]^+$.

4.1.49. 5-(4-((1-isobutyl-1*H*-benzo[*d*]imidazol-2-yl)methoxy)benzyl)thiazolidine-2,4-dione (5b)

The title compound was prepared from the respective knoevenagel product **21b** following the same procedure used for the preparation of **5a.** Flash column purification (100% DCM to DCM/MeOH; 96:4 stepwise gradient) afforded the desired end product as a yellow sticky solid (0.21 g). Yield: 85%; mp: 173-175 °C; ^{1}H-NMR (300 MHz, DMSO-d_6): δ 0.79-0.89 (m, 6H), 2.21-2.33 (m, 1H), 3.06 (dd, *J* = 9.16, 14.04 Hz, 1H), 3.31 (dd, *J* = 4.27, 14.04 Hz, 1H), 4.12 (d, *J* = 7.81 Hz, 2H), 4.87 (dd, *J* = 4.27, 9.16 Hz, 1H), 5.36 (s, 2H), 6.97-7.09 (m, 2H), 7.14-7.31 (m, 4H), 7.61 (d, *J* = 7.57 Hz, 1H), 7.66 (d, *J* = 7.57 Hz, 1H), 12.17 (br s, 1H); ^{13}C-NMR (300 MHz, DMSO-d_6): δ 19.79, 28.63, 36.29, 50.39, 52.88, 62.44, 110.86, 114.48,

119.12, 121.50, 122.43, 130.15, 132.56, 141.54, 147.12, 149.24, 156.62, 171.35, 175.46; MS (ESI^+) *m/z*: 410 $[M+H]^+$.

4.1.50. 5-(4-((1-allyl-1*H*-benzo[*d*]imidazol-2-yl)methoxy)benzyl)thiazolidine-2,4-dione (5c)

Reduction of the respective Knoevenagel product **21c** (0.25 g, 0.64 mmol) was achieved by a method similar to that described for **5a**. The title end product was afforded as a yellowish white solid (0.18 g). Yield: 71%; mp: >300 °C; ^{1}H-NMR (400 MHz, DMSO-d_6): δ 3.07 (dd, *J* = 9.17, 14.18 Hz, 1H), 3.32 (dd, *J* = 4.28, 14.18 Hz, 1H), 4.88 (dd, *J* = 4.28, 9.17 Hz, 1H), 4.97 (d, *J* = 5.38 Hz, 2H), 5.05 (d, *J* = 17.85 Hz, 1H), 5.18 (d, *J* = 10.27 Hz, 1H), 5.37 (s, 2H), 5.90-6.06 (m, 1H), 7.06 (d, *J* = 8.56 Hz, 2H), 7.20 (d, *J* = 8.56 Hz, 2H), 7.22-7.32 (m, 2H), 7.52-7.61 (m, 1H), 7.68 (d, *J* = 7.83 Hz, 1H), 12.11 (br s, 1H); ^{13}C-NMR (400 MHz, DMSO-d_6): δ 36.79, 46.37, 53.42, 63.01, 111.21, 115.19, 117.88, 119.91, 122.39, 123.31, 130.00, 130.87, 133.50, 142.36, 149.82, 157.35, 172.13, 176.17; MS (ESI^+) *m/z*: 394 $[M+H]^+$.

4.1.51. 5-(4-((1-isopropyl-1*H*-benzo[*d*]imidazol-2-yl) methoxy) benzyl) thiazolidine-2,4-dione (5d)

Reduction of the respective Knoevenagel product **21d** (0.25 g, 0.64 mmol) was performed by a method similar to that described for **5a**. The title end product was obtained as yellowish white solid (0.17 g). Yield: 66%; mp: 185-187 °C; ^{1}H-NMR (300 MHz, DMSO-d_6): δ 1.47-1.64 (m, 6H), 3.06 (dd, *J* = 9.28, 14.28 Hz, 1H), 3.33 (dd, *J* = 4.27, 14.28 Hz, 1H), 4.63 (dd, *J* = 4.27, 9.28 Hz, 1H), 4.85 (m, 1H), 5.39 (s, 2H), 6.95-7.10 (m, 2H), 7.11-7.33 (m, 4H), 7.61-7.69 (m, 1H), 7.74 (dd, *J* = 1.71, 6.84 Hz, 1H), 12.19 (br s, 1H); ^{13}C-NMR (300 MHz, DMSO-d_6): δ 20.94, 36.28, 48.07, 52.83, 62.85, 112.22, 114.52, 119.54, 121.24, 122.26, 129.31, 130.15, 142.59, 149.73, 156.52, 171.28, 175.34; MS (ESI^+) *m/z*: 396 $[M+H]^+$.

4.1.52. 5-(4-((1-cyclopentyl-1*H*-benzo[*d*]imidazol-2-yl)methoxy)benzyl)thiazolidine-2,4-dione (5e)

Reduction of the respective Knoevenagel product **21e** (0.25 g, 0.60 mmol) was achieved by a method similar to that described for **1a**. The title end product was afforded as a yellowish white solid (0.19 g). Yield: 75%; mp: >300 °C; ^{1}H-NMR (300 MHz, DMSO-d_6): δ 1.73-1.79 (m, 2H), 1.99-2.07 (m, 2H), 2.15-2.25 (m, 4H), 3.11(dd, J = 8.79, 14.38 Hz, 1H), 3.31 (dd, J = 3.91, 14.38 Hz, 1H), 4.89 (dd, J = 3.91, 8.79 Hz, 1H), 5.12 (m, 1H), 5.67 (s, 2H), 7.14 (d, J = 8.55 Hz, 2H), 7.23 (d, J = 8.55 Hz, 2H), 7.42-7.54 (m, 2H), 7.76-7.92 (m, 2H), 12.06 (s, 1H); ^{13}C-NMR (300 MHz, DMSO-d_6): δ 24.40, 29.71, 36.18, 52.73, 57.63, 61.33, 113.37, 114.74, 116.58, 124.57, 125.32, 129.92, 130.28, 132.35, 144.81, 148.71, 156.01, 171.23, 175.29; MS (ESI$^+$) *m/z*: 422 $[M+H]^+$.

4.2. Biological evaluation

4.2.1. PPARγ Functional reporter gene assay

The PPARγ functional assay was performed at Indigo Biosciences Inc., State College, PA, USA. A suspension of Reporter Cells was prepared in Cell Recovery Medium (CRM; containing 10% charcoal stripped FBS). The reporter cells used in this assay express a hybrid receptor comprising the N-terminal Gal4 DNA binding domain fused to the ligand binding domain of Human PPARγ. The reporter vectors comprise the firefly luciferase gene functionally linked to the Gal4 upstream activation sequence (UAS). 100 µl of the Reporter Cell suspension was dispensed into wells of a white 96-well assay plate. Immediately prior to assay setup, test compounds were diluted using compound screening medium (CSM; containing 10% charcoal stripped FBS) to generate 2x-concentration treatment media. 100 µl of each treatment medium was dispensed into triplicate assay wells pre-dispensed with Reporter Cells. Assay plates were incubated at 37°C for 24 h. Following the incubation

period, treatment media were discarded and 100 µl/well of Luciferase Detection Reagent was added. RLUs were quantified from each assay well to determine nuclear receptor activities. Dose-response curve (DRC) analyses of reference compounds were performed via non-linear curve-fitting of RLU vs. Log[Cmpd] using GraphPad Prism software.

4.2.2. FFAR1 functional β-Arrestin assay

CHO-K1 cells expressing FFAR1 receptor were seeded in a 384-well black-wall, clear bottom plate at a density of 15,000 cells per well in 20 µl of growth medium,18 hours prior to the day of experiment and maintained at 37 °C in 5% CO_2. 20 µl of dye-loading solution was added into the wells. Then the plate was placed into a 37°C incubator for 60 minutes, followed by a 15 minutes at room temperature. At last, 10 µl compounds or control agonist were added into respective wells of the assay plate during reading in FLIPR. Compounds or control were added to the reading plate at 20 sec and the fluorescence signal was monitored for an additional 100 sec (21 sec to 120 sec.). Data were recorded by ScreenWorks (version 3.1) as FMD files with FLIPR. Data acquisition and analyses was performed using ScreenWorks (version 3.1) program and exported to Excel. Dose response curves of agonist were fitted from four parameter logistic equation by the software GraphPad Prism.

4.4. Docking

All the compounds were built and energy-minimized using MMFF charges and the MMFF force field as implemented in Sybyl X.1 with 2000 steps of the conjugate gradient method to a gradient of 0.001 kcal/Å.[57] CCDC GOLD 4.12 software was used for docking of the minimized compounds into the binding pocket of the X-ray crystal structures of PPARγ and FFAR1.[58] This software uses a genetic algorithm (GA) to explore possible ligand binding modes by changing dihedrals of ligand rotatable bonds, ligand ring geometries, and dihedrals of protein OH and NH_2 groups.[59] The binding site was defined to include all amino acid

residues within 10 Å of the side chain nitrogen of Arg258 with H bond constraint to its side chain NH. Docking was carried out using the standard mode settings and GoldScore, a molecular mechanics-like function depending on protein-ligand hydrogen bonding, protein-ligand van der Waals score, ligand intramolecular hydrogen bonding, and ligand intramolecular strain.[60] A total of 10 genetic algorithm runs were performed for each ligand with early termination criteria set to 1.5 Å root-mean-square deviation (RMSD) value.

Acknowledgement

This study was entirely funded by the Science and Technology Development Fund (STDF), Egypt, Grant #4244, awarded to the Principal Investigator Dr. Mohamed A. Helal. The authors would like to thank Dr. Safwat A. Ahmad, Pharmacognosy Department, Faculty of Pharmacy, Suez Canal University, for providing access to some necessary laboratory equipment. The authors would also like to thank Dr. Mohamed Saleh Elgawish, Graduate School of Biomedical Sciences, Course of Pharmaceutical Sciences, Nagasaki University, 1-14 Bunkyo-machi, Nagasaki 852-8521, Japan, for performing mass and specific rotation measurements.

Supplementary data

Supplementary data associated with this article can be found, in the online version.

References and notes

[1] F.S.B. National Institute of Diabetes and Digestive and Kidney Diseases. National Diabetes Statistics, MD: U.S. Department of Health and Human Services, National Institutes of Health, 2008., in.

[2] I.D.F. (IDF), Diabetes atlas, in, 2010.

[3] F. Wang, Z. Liu, J. Wang, J. Tao, P. Gong, X. Bao, Y. Zhao, Y. Wang, The interaction of 4-thiazolidinone derivatives containing indolin-2-one moiety with P-glycoprotein studied using K562 cell lines, Eur J Med Chem, 101 (2015) 126-132.

[4] D. Havrylyuk, B. Zimenkovsky, O. Karpenko, P. Grellier, R. Lesyk, Synthesis of pyrazoline-thiazolidinone hybrids with trypanocidal activity, Eur J Med Chem, 85 (2014) 245-254.

[5] K.S. Sharath Kumar, A. Hanumappa, M. Hegde, K.H. Narasimhamurthy, S.C. Raghavan, K.S. Rangappa, Synthesis and antiproliferative effect of novel 4-thiazolidinone-, pyridine- and piperazine-based conjugates on human leukemic cells, Eur J Med Chem, 81 (2014) 341-349.

[6] Z.H. Zhao, Y.C. Fan, Q. Zhao, C.Y. Dou, X.F. Ji, J. Zhao, S. Gao, X.Y. Li, K. Wang, Promoter methylation status and expression of PPAR-gamma gene are associated with prognosis of acute-on-chronic hepatitis B liver failure, Clinical epigenetics, 7 (2015) 115.

[7] S. Kersten, B. Desvergne, W. Wahli, Roles of PPARs in health and disease, Nature, 405 (2000) 421-424.

[8] S. Costanzi, S. Neumann, M.C. Gershengorn, Seven transmembrane-spanning receptors for free fatty acids as therapeutic targets for diabetes mellitus: pharmacological, phylogenetic, and drug discovery aspects, J Biol Chem, 283 (2008) 16269-16273.

[9] T. Hara, A. Hirasawa, A. Ichimura, I. Kimura, G. Tsujimoto, Free fatty acid receptors FFAR1 and GPR120 as novel therapeutic targets for metabolic disorders, J Pharm Sci, 100 (2011) 3594-3601.

[10] M.A.R. G. C. CHERFAN, MIDDLE EAST MEDICAL INDEX, in, CCM MIDDLE EAST s.a.r.l., 2011.

[11] K. Kotarsky, N.E. Nilsson, E. Flodgren, C. Owman, B. Olde, A human cell surface receptor activated by free fatty acids and thiazolidinedione drugs, Biochem Biophys Res Commun, 301 (2003) 406-410.

[12] C.O. Owman, Bjorn; Kotarsky, Knut; Nilsson, Niclas; Flodgren, Erik. . Methods of identifying compounds that affect a fatty acid cell-surface receptor. U.S. Pat. Appl. Publ. (2004), 19 pp. CODEN: USXXCO US 2004019109 A1 20040129 CAN 140:139513 AN 2004:80358 CAPLUS, in.

[13] O.B. Owman Christer, Rome Daniel, Sterner Olov, Therapeutic modulators of GPR40, in, USA, 2007.

[14] C.P. Tan, Y. Feng, Y.P. Zhou, G.J. Eiermann, A. Petrov, C. Zhou, S. Lin, G. Salituro, P. Meinke, R. Mosley, T.E. Akiyama, M. Einstein, S. Kumar, J.P. Berger, S.G. Mills, N.A. Thornberry, L. Yang, A.D. Howard, Selective small-molecule agonists of G protein-coupled receptor 40 promote glucose-dependent insulin secretion and reduce blood glucose in mice, Diabetes, 57 (2008) 2211-2219.

[15] http://clinicaltrials.gov/ct2/show/NCT00388518, in.

[16] R.S. McIntyre, Pharmacology and efficacy of asenapine for manic and mixed states in adults with bipolar disorder, Expert Rev Neurother, 10 (2010) 645-649.

[17] S. Aleshin, M. Strokin, M. Sergeeva, G. Reiser, Peroxisome proliferator-activated receptor (PPAR)β/δ, a possible nexus of PPARα- and PPARγ-dependent molecular

pathways in neurodegenerative diseases: Review and novel hypotheses, Neurochem Int, 63 (2013) 322-330.
[18] C. Lamers, M. Schubert-Zsilavecz, D. Merk, Therapeutic modulators of peroxisome proliferator-activated receptors (PPAR): a patent review (2008-present), Expert Opin Ther Pat, 22 (2012) 803-841.
[19] X.T. Feng, J. Leng, Z. Xie, S.L. Li, W. Zhao, Q.L. Tang, GPR40: a therapeutic target for mediating insulin secretion (review), Int J Mol Med, 30 (2012) 1261-1266.
[20] R. Chen, J. Yan, P. Liu, Z. Wang, Effects of thiazolidinedione therapy on inflammatory markers of type 2 diabetes: a meta-analysis of randomized controlled trials, PLoS One, 10 (2015) e0123703.
[21] H.T. Tseng, Y.J. Park, Y.K. Lee, D.D. Moore, The orphan nuclear receptor small heterodimer partner is required for thiazolidinedione effects in leptin-deficient mice, Journal of biomedical science, 22 (2015) 30.
[22] R.K. Sharma, Y. Younis, G. Mugumbate, M. Njoroge, J. Gut, P.J. Rosenthal, K. Chibale, Synthesis and structure-activity-relationship studies of thiazolidinediones as antiplasmodial inhibitors of the Plasmodium falciparum cysteine protease falcipain-2, Eur J Med Chem, 90 (2015) 507-518.
[23] M.A. Helal, K.M. Darwish, M.A. Hammad, Homology modeling and explicit membrane molecular dynamics simulation to delineate the mode of binding of thiazolidinediones into FFAR1 and the mechanism of receptor activation, Bioorg Med Chem Lett, 24 (2014) 5330-5336.
[24] B.E. Evans, K.E. Rittle, M.G. Bock, R.M. DiPardo, R.M. Freidinger, W.L. Whitter, G.F. Lundell, D.F. Veber, P.S. Anderson, R.S. Chang, et al., Methods for drug discovery: development of potent, selective, orally effective cholecystokinin antagonists, J Med Chem, 31 (1988) 2235-2246.
[25] G.W. Bemis, M.A. Murcko, The properties of known drugs. 1. Molecular frameworks, J Med Chem, 39 (1996) 2887-2893.
[26] X.Q. Lewell, D.B. Judd, S.P. Watson, M.M. Hann, RECAP--retrosynthetic combinatorial analysis procedure: a powerful new technique for identifying privileged molecular fragments with useful applications in combinatorial chemistry, J Chem Inf Comput Sci, 38 (1998) 511-522.
[27] a.M.D.M. Robert P. Sheridan, A method of visualizing recurrent topological substructures in sets of active molecules, Journal of Chemical Information and Modeling, 38 (1998) 915-924.
[28] R.W. DeSimone, K.S. Currie, S.A. Mitchell, J.W. Darrow, D.A. Pippin, Privileged structures: applications in drug discovery, Comb Chem High Throughput Screen, 7 (2004) 473-494.
[29] K.V. Balakin, S.E. Tkachenko, S.A. Lang, I. Okun, A.A. Ivashchenko, N.P. Savchuk, Property-based design of GPCR-targeted library, J Chem Inf Comput Sci, 42 (2002) 1332-1342.
[30] L. Costantino, D. Barlocco, Privileged structures as leads in medicinal chemistry, Curr Med Chem, 13 (2006) 65-85.
[31] L. De Luca, Naturally occurring and synthetic imidazoles: their chemistry and their biological activities, Curr Med Chem, 13 (2006) 1-23.
[32] C.D. Duarte, E.J. Barreiro, C.A. Fraga, Privileged structures: a useful concept for the rational design of new lead drug candidates, Mini Rev Med Chem, 7 (2007) 1108-1119.
[33] M. Kato, A. Furuno, N. Shimizu, Characterization of S1 nuclease-sensitive structure of the pyrimidine/purine biased sequence in promoter region of the human EGF receptor gene, Nucleic Acids Symp Ser, (1991) 35-36.

[34] F. Song, S. Lu, J. Gunnet, J.Z. Xu, P. Wines, J. Proost, Y. Liang, C. Baumann, J. Lenhard, W.V. Murray, K.T. Demarest, G.H. Kuo, Synthesis and biological evaluation of 3-aryl-3-(4-phenoxy)-propionic acid as a novel series of G protein-coupled receptor 40 agonists, J Med Chem, 50 (2007) 2807-2817.

[35] S. Mikami, S. Kitamura, N. Negoro, S. Sasaki, M. Suzuki, Y. Tsujihata, T. Miyazaki, R. Ito, N. Suzuki, J. Miyazaki, T. Santou, N. Kanzaki, M. Funami, T. Tanaka, T. Yasuma, Y. Momose, Discovery of phenylpropanoic acid derivatives containing polar functionalities as potent and orally bioavailable G protein-coupled receptor 40 agonists for the treatment of type 2 diabetes, J Med Chem, 55 (2012) 3756-3776.

[36] T. Izumi, F. Tsuruta, T. Ishizuka, K. Nakamura, M. Kothuma, M. Takahashi, Stereoselectivity in pharmacokinetics of rivoglitazone, a novel peroxisome proliferator-activated receptor γ agonist, in rats and monkeys: model-based pharmacokinetic analysis and in vitro-in vivo extrapolation approach, J Pharm Sci, 102 (2013) 3174-3188.

[37] A. Menteşe, M. Ceylan-Unlüsoy, O. Bozdağ-Dündar, N. Altanlar, R. Ertan, Synthesis and antimicrobial activity of some novel thiazolidine-2,4-dione derivatives, Arzneimittelforschung, 59 (2009) 659-665.

[38] O. Sugimoto, T. Arakaki, H. Kamio, K. Tanji, The use of a Mitsunobu reagent for the formation of heterocycles: a simple method for the preparation of 3-alkyl-5-aryl-1,3,4-oxadiazol-2(3H)-ones from carboxylic acids, Chem Commun (Camb), 50 (2014) 7314-7317.

[39] D.B. Ramachary, K. Anebouselvy, N.S. Chowdari, C.F. Barbas, Direct organocatalytic asymmetric heterodomino reactions: the Knoevenagel/Diels-Alder/epimerization sequence for the highly diastereoselective synthesis of symmetrical and nonsymmetrical synthons of benzoannelated centropolyquinanes, J Org Chem, 69 (2004) 5838-5849.

[40] M.A. Düfert, K.L. Billingsley, S.L. Buchwald, Suzuki-Miyaura cross-coupling of unprotected, nitrogen-rich heterocycles: substrate scope and mechanistic investigation, J Am Chem Soc, 135 (2013) 12877-12885.

[41] D.C. Lacy, C.C. McCrory, J.C. Peters, Studies of cobalt-mediated electrocatalytic CO2 reduction using a redox-active ligand, Inorg Chem, 53 (2014) 4980-4988.

[42] L. Deloux, Srebnik, M., Asymmetric boron-catayzed reactions., Chem Rev., 93 (1993) 763-784.

[43] H. Zhu, D.J. O'Leary, M.P. Meyer, Stereoselection in the Corey-Bakshi-Shibata reduction: insight from kinetic isotope effects and transition-structure modeling, Angew Chem Int Ed Engl, 51 (2012) 11890-11893.

[44] W. Lu, S. Sengupta, J.L. Petersen, N.G. Akhmedov, X. Shi, Mitsunobu coupling of nucleobases and alcohols: an efficient, practical synthesis for novel nonsugar carbon nucleosides, J Org Chem, 72 (2007) 5012-5015.

[45] E. Westman, R. Stromberg, Removal of t-butyldimethylsilyl protection in RNA-synthesis. Triethylamine trihydrofluoride (TEA, 3HF) is a more reliable alternative to tetrabutylammonium fluoride (TBAF), Nucleic Acids Res, 22 (1994) 2430-2431.

[46] C. Huang, V. Gevorgyan, TBDPS and Br-TBDPS protecting groups as efficient aryl group donors in Pd-catalyzed arylation of phenols and anilines, J Am Chem Soc, 131 (2009) 10844-10845.

[47] I.G. Tikhonova, C.S. Sum, S. Neumann, S. Engel, B.M. Raaka, S. Costanzi, M.C. Gershengorn, Discovery of novel agonists and antagonists of the free fatty acid receptor 1 (FFAR1) using virtual screening, J Med Chem, 51 (2008) 625-633.

[48] C.G. Walker, L. Goff, L.J. Bluck, B.A. Griffin, S.A. Jebb, J.A. Lovegrove, T.A. Sanders, G.S. Frost, Variation in the FFAR1 gene modifies BMI, body composition and beta-cell function in overweight subjects: an exploratory analysis, PLoS One, 6 (2011) e19146.

[49] H. Elshihawy, M.A. Helal, M. Said, M.A. Hammad, Design, synthesis, and enzyme kinetics of novel benzimidazole and quinoxaline derivatives as methionine synthase inhibitors, Bioorg Med Chem, 22 (2014) 550-558.
[50] H. Kojo, M. Fukagawa, K. Tajima, A. Suzuki, T. Fujimura, I. Aramori, K. Hayashi, S. Nishimura, Evaluation of human peroxisome proliferator-activated receptor (PPAR) subtype selectivity of a variety of anti-inflammatory drugs based on a novel assay for PPAR delta(beta), J Pharmacol Sci, 93 (2003) 347-355.
[51] B.R. Kumar, M.J. Nanjan, Novel glitazones: design, synthesis, glucose uptake and structure-activity relationships, Bioorg Med Chem Lett, 20 (2010) 1953-1956.
[52] Y. Zhang, D. Kowal, A. Kramer, J. Dunlop, Evaluation of FLIPR Calcium 3 Assay Kit--a new no-wash fluorescence calcium indicator reagent, J Biomol Screen, 8 (2003) 571-577.
[53] C. Pirat, A. Farce, N. Lebègue, N. Renault, C. Furman, R. Millet, S. Yous, S. Speca, P. Berthelot, P. Desreumaux, P. Chavatte, Targeting peroxisome proliferator-activated receptors (PPARs): development of modulators, J Med Chem, 55 (2012) 4027-4061.
[54] V. Chandra, P. Huang, Y. Hamuro, S. Raghuram, Y. Wang, T.P. Burris, F. Rastinejad, Structure of the intact PPAR-gamma-RXR- nuclear receptor complex on DNA, Nature, 456 (2008) 350-356.
[55] P. Markt, R.K. Petersen, E.N. Flindt, K. Kristiansen, J. Kirchmair, G. Spitzer, S. Distinto, D. Schuster, G. Wolber, C. Laggner, T. Langer, Discovery of novel PPAR ligands by a virtual screening approach based on pharmacophore modeling, 3D shape, and electrostatic similarity screening, J Med Chem, 51 (2008) 6303-6317.
[56] A. Srivastava, J. Yano, Y. Hirozane, G. Kefala, F. Gruswitz, G. Snell, W. Lane, A. Ivetac, K. Aertgeerts, J. Nguyen, A. Jennings, K. Okada, High-resolution structure of the human GPR40 receptor bound to allosteric agonist TAK-875, Nature, 513 (2014) 124-127.
[57] A. Cheng, S.A. Best, K.M. Merz, Jr., C.H. Reynolds, GB/SA water model for the Merck molecular force field (MMFF), J Mol Graph Model, 18 (2000) 273-282.
[58] G. Jones, P. Willett, R.C. Glen, A.R. Leach, R. Taylor, Development and validation of a genetic algorithm for flexible docking, J Mol Biol, 267 (1997) 727-748.
[59] M.A. Helal, S. Khalifa, S. Ahmed, Differential binding of latrunculins to G-actin: a molecular dynamics study, J Chem Inf Model, 53 (2013) 2369-2375.
[60] M.K. Annamala, K.K. Inampudi, L. Guruprasad, Docking of phosphonate and trehalose analog inhibitors into M. tuberculosis mycolyltransferase Ag85C: Comparison of the two scoring fitness functions GoldScore and ChemScore, in the GOLD software, Bioinformation, 1 (2007) 339-350.

List of Captions:

Figure 1: TZD-fatty acid hybrids.

Figure 2: Representative examples of FFAR1 agonists and PPARγ agonists.

Figure 3: Design strategy of the dual PPARγ/FFAR1 agonists.

Figure 4: Scaffolds with the highest docking score in both FFAR1 and PPARγ.

Scheme 1: (**a**) $ClCH_2COOH$, H_2O, rt, 30 min; (**b**) 4-Hydroxybenzaldehyde, piperidine, benzoic acid, toluene reflux, 16 h; (**c**) benzyl chloride, Cs_2CO_3, DMF, rt, 4 h; (**d**) 1 M NaOH, $CoCl_2$-DMG, $NaHB_4$, THF, 35-40 °C, 16 h.

Scheme 2: (**a**) 4-Hydroxybenzaldehyde, Ph_3P, DIAD, THF, 0ºC to rt, 16 h; (**b**) $ArB(OH)_2$, $Pd(PPh_3)_4$, Na_2CO_3, toluene, reflux, 16 h; (**c**) 1,3-thiazolidine-2,4-dione, piperidine, benzoic acid, toluene, reflux, 16 h; (**d**) 1 M NaOH, $CoCl_2$-DMG, $NaHB_4$, THF, 35-40 °C, 16 h.

Scheme 3: (**a**) (S)-oxazaborolidine, BH_3•THF, Toluene, rt, 90 min; (**b**) 4-Hydroxybenzaldehyde, Cs_2CO_3, DMF/THF, 50 ºC, 16 h; (**c**) 4-Hydroxybenzaldehyde, Ph_3P, DIAD, THF, 0ºC to rt, 16 h; (**d**) 1,3-thiazolidine-2,4-dione, piperidine, benzoic acid, toluene, reflux, 16 h; (**e**) 1 M NaOH, $CoCl_2$-DMG, $NaHB_4$, THF, 35-40 °C, 16 h.

Scheme 4: (**a**) 67% w/v glycolic acid, 6 N HCl, reflux, 16 h; (**b**) RCl, NaH, anhydrous DMF, 0 °C to rt, 16 h;. (**c**) 4-Hydroxybenzaldehyde, Ph_3P, DIAD, THF, 0ºC to rt, 16 h; (**d**) 1,3-thiazolidine-2,4-dione, piperidine, benzoic acid, toluene, reflux, 16 h; (**e**) 1 M NaOH, $CoCl_2$-DMG, $NaHB_4$, THF, 35-40 °C, 16 h.

Figure 5: Proposed binding mode of **1a (a), 2d (b),** and **5b** in the crystal structure of PPARγ. Protein is represented as grey cartoon with amino acid residue colored green. Compounds are displayed as yellow sticks. Only residues having significant interaction with the ligand are shown.

Figure 6: Proposed binding mode of **1a (a), 2g (b),** and **5b** in the crystal structure of FFAR1. Protein is represented as grey cartoon with amino acid residue colored green. The crystallized ligand TAK-875 (cyan) and the prepared compound (yellow) are displayed as sticks. A part of TM4 was removed for clarity.

Table 1: *In vitro* data of the human PPAR-γ transactivation assay.[a]

Compound	*R Group*	Fold-induction[b]		EC_{50} (μM)[c]
		Compared to vehicle (1 fold)	Percentage compared to Rosiglitazone	
Vehicle	NA	1	2.3	–
Rosiglitazone	NA	43	100%	0.24
5	NA	11	34.9	ND
11a	NA	38	88.4	25.21
11b	NA	40	93.0	17.03
1a	H	15	34.9	ND
1b	2-Me	5.4	12.6	ND
1c	2,6-DiMe	3.5	8.1	ND
1d	4-CF_3	0.24	0.1	ND
2a	H	1.1	2.6	ND
2b	3-Me	3.5	8.1	ND
2c	4-Me	3.9	9.1	ND
2d	3-OMe	5	11.6	ND
2e	4-CF_3	1.1	2.6	ND
2f	4-Cl	2.3	5.3	ND
2g	2,4-DiCl	1.8	4.2	ND
5a	Benzyl	29	67.4	30.23
5b	Isobutyl	24	55.8	13.21
5c	Allyl	55	127.9	4.93
5d	Isopropyl	29	67.4	25.41
5e	Cyclopentyl	3.7	8.6	ND

[a] Reported *in vitro* values are the average of two replicates, NA denotes not applicable.
[b] Fold-induction values for the prepared compounds were obtained at 30 μM and calculated relative to that of the vehicle (DMSO 0.10%) and as percentage of the obtained fold-induction with the reference compound rosiglitazone.
[c] EC_{50} value represents the effective concentration for 50% response of a given compound's intrinsic maximum response; ND denotes not determined.

Table 2: *In vitro* data for the human FFAR1 calcium flux FLIPR assay.[a]

Compound	R group	EC_{50} (μM)
γ-linolenic acid	NA	4.62
5	NA	6.56
11a	NA	3.57
11b	NA	23.12
1a	H	9.91
1b	2-Me	7.73
1c	2,6-DiMe	1.15
1d	4-CF3	6.11
2a	H	IA
2b	3-Me	IA
2c	4-Me	IA
2d	3-OMe	19.58
2e	4-CF_3	7.42
2f	4-Cl	8.51
2g	2,4-DiCl	1.66
5a	Benzyl	4.11
5b	Isobutyl	1.89
5c	Allyl	21.01
5d	Isopropyl	16.60
5e	Cyclopentyl	IA

[a] Reported *in vitro* values are the average of two replicates.

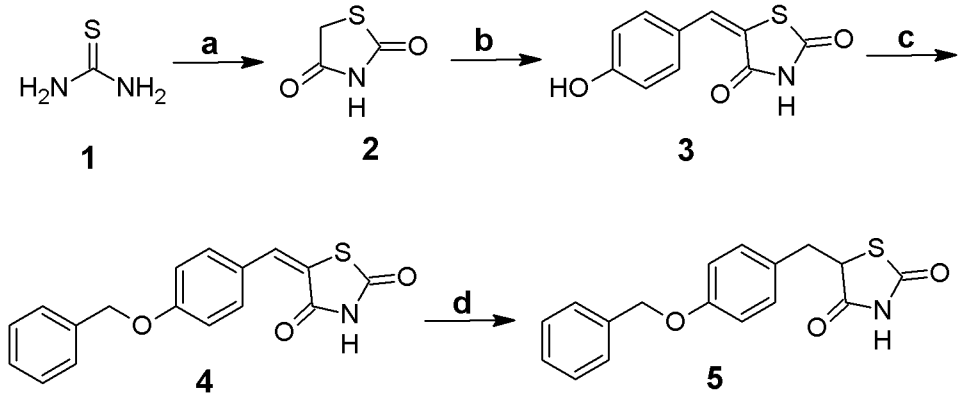

1 2 3

4 5

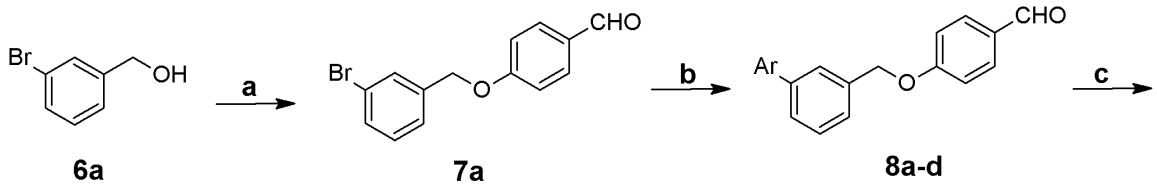

6a **7a** **8a-d**

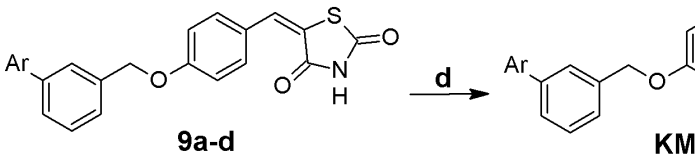

9a-d **KM-1a-d**

a, Ar = Ph
b, Ar = 2-Me-Ph
c, Ar = 2,6-diMe-Ph
d, Ar = 4-CF_3-Ph

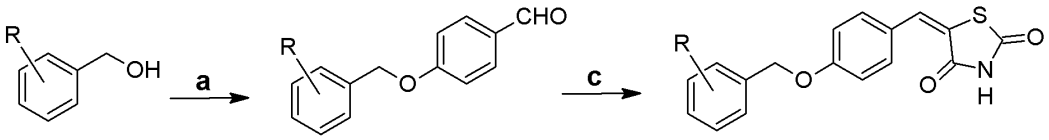

6a,b **7a,b** **10a,b**

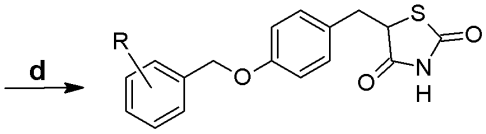

11a,b

a, R = 3-Br
b, R = 4-Br

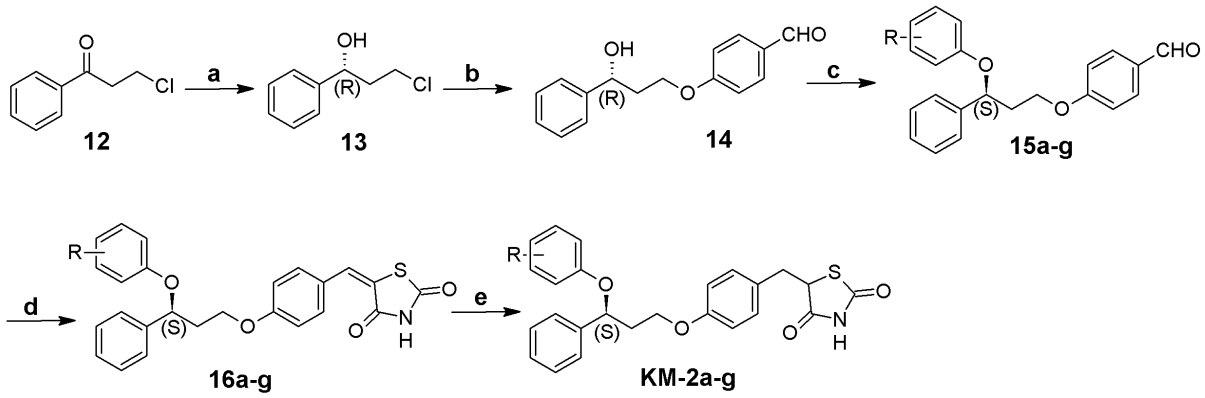

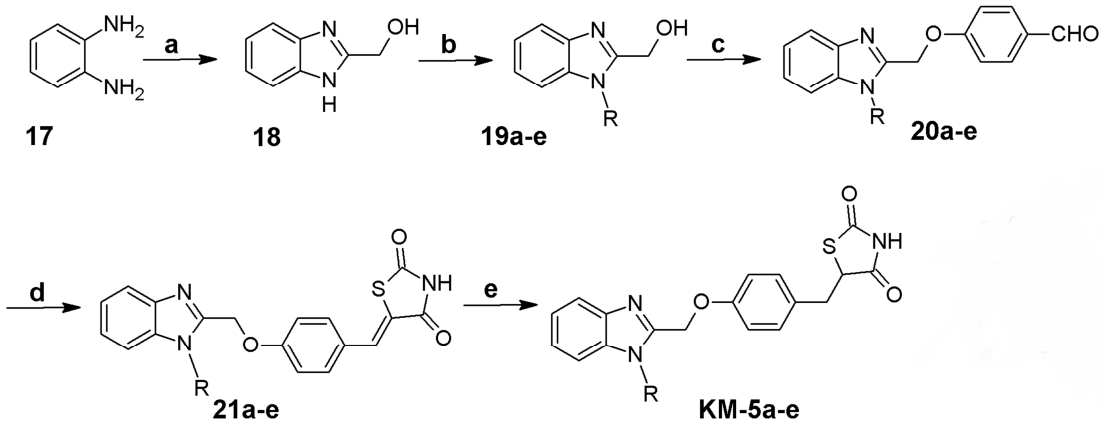

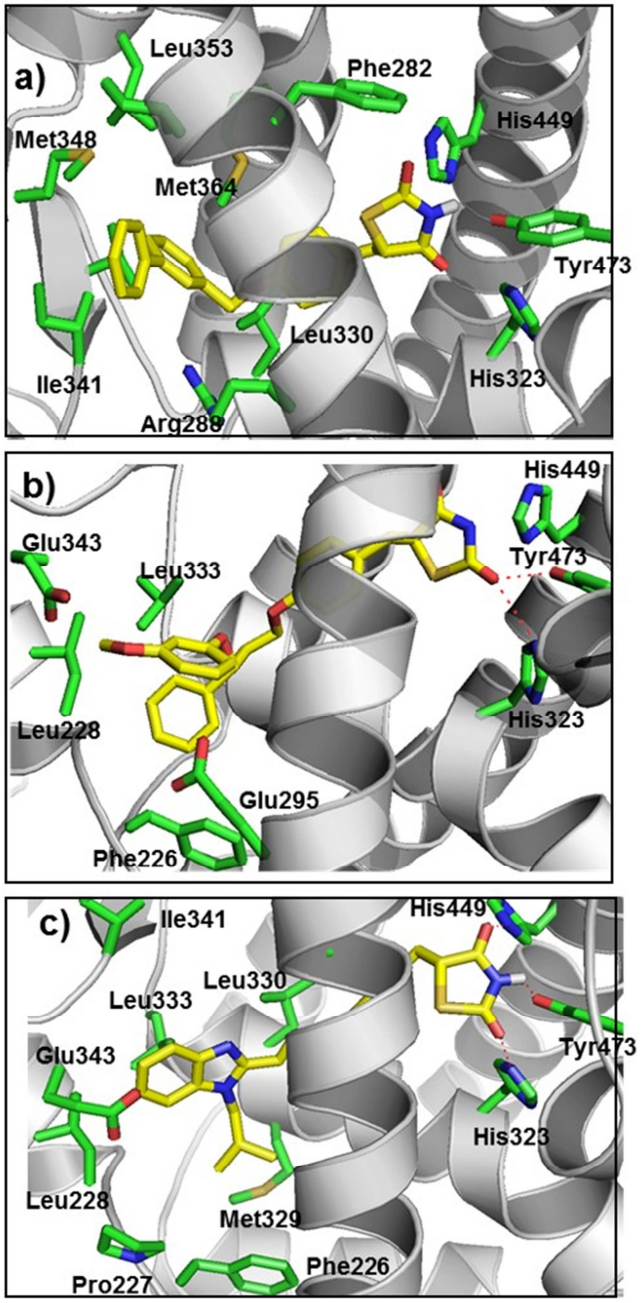

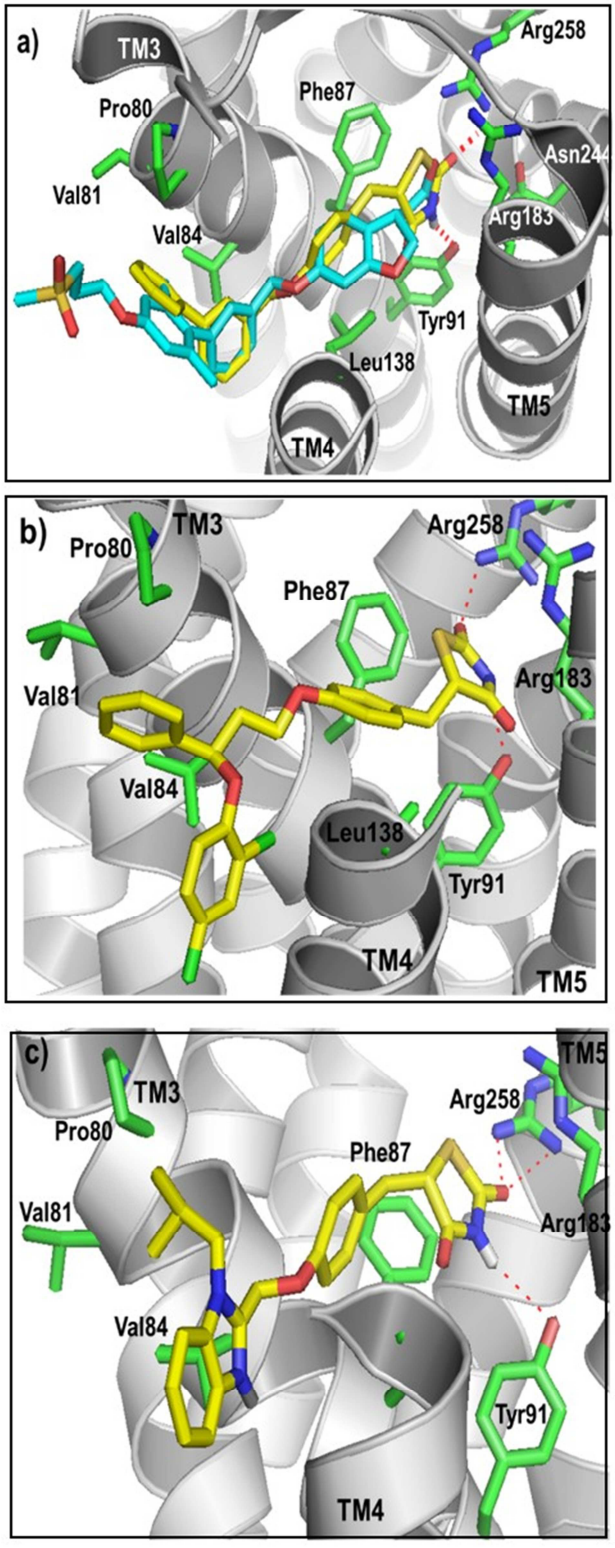
a)
TM3
Arg258
Phe87
Pro80
Asn244
Val81
Arg183
Val84
Tyr91
Leu138
TM5
TM4
b)
Pro80
TM3
Arg258
Phe87
Arg183
Val81
Val84
Leu138
Tyr91
TM4
TM5
c)
TM5
TM3
Arg258
Pro80
Phe87
Val81
Arg183
Val84
Tyr91
TM4

Highlights

Design, Synthesis, and Biological Evaluation of Novel Thiazolidinediones as PPARγ/FFAR1 Dual Agonists

Khalid M. Darwish[a], Ismail Salama[a], Samia M. Mostafa[a], Mohamed S. Gomaa[a], and Mohamed A. Helal[a,*]
[a] Medicinal Chemistry Department, Faculty of Pharmacy, Suez Canal University, Ismailia 41522, Egypt.

Corresponding Author: Mohamed A. Helal
Tel: +201201122213
E-mail address: mohamed_hilal@pharm.suez.edu.eg

- PPARγ and FFAR1 are valid targets for the management of type 2 diabetes.
- Some thiazolidinediones (PPAR ligands) could activate FFAR1 with micromolar potency.
- In this study, nineteen dual PPARγ/FFAR1 agonists were designed.
- The design depends on using TZD head with diverse privileged structures.
- Nine compounds showed promising dual activity.